

1 **HY5 regulates GLK and GNC transcription factors to**  
2 **orchestrate photomorphogenesis in *Arabidopsis***  
3 ***thaliana***

4  
5 **Ting Zhang<sup>1,2,5</sup>, Rui Zhang<sup>1,5</sup>, Xi-Yu Zeng<sup>1,2,5</sup>, Lu-Huan Ye<sup>1</sup>, Shi-Long Tian<sup>2</sup>,**  
6 **Yi-Jing Zhang<sup>3</sup>, Wen-Bin Zhou<sup>4</sup>, Xin-Guang Zhu<sup>1</sup>, Peng Wang<sup>1,\*</sup>**

7  
8 1 Laboratory of Photosynthesis and Environmental Biology, CAS Center for  
9 Excellence in Molecular Plant Sciences (CEMPS), Chinese Academy of  
10 Sciences, Shanghai 200032, China

11 2 University of Chinese Academy of Sciences, Shanghai 200032, China

12 3 State Key Laboratory of Genetic Engineering, Collaborative Innovation Center  
13 of Genetics and Development, Department of Biochemistry, Institute of Plant  
14 Biology, School of Life Sciences, Fudan University, Shanghai 200438, China

15 4 Institute of Crop Sciences, Chinese Academy of Agricultural Sciences, Beijing  
16 100081, China

17 5 These authors contributed equally to this work

18

19 \* Author for correspondence: wangpeng@cemps.ac.cn (P.W.)

20

21 T.Z. and P.W. designed the study. T.Z. and R.Z. performed most of the  
22 experiments. X.-Y.Z. worked on the transcriptional activation and protein  
23 interaction. L.-H.Y. worked on the ChIP-qPCR experiments. S.-L.T. analyzed the  
24 RNA-seq data. P.W., Y.-J.Z., W.-B.Z., and X.-G.Z. wrote and revised the  
25 manuscript.

26

27 **Short title:** GLK and GNC regulate photomorphogenesis

28

29 **One-sentence summary:** GLK and GNC act downstream of HY5, and cooperate  
30 with HY5 and DET1, to regulate both chloroplast development and hypocotyl  
31 elongation during the transition from skotomorphogenesis to  
32 photomorphogenesis.

33

34

35

36

37 **Abstract**

38 Light induced de-etiolation is an important aspect of seedling  
39 photomorphogenesis. GOLDEN2 LIKE (GLK) and GATA NITRATE-INDUCIBLE  
40 CARBON-METABOLISM-INVOLVED (GNC) are master transcriptional regulators  
41 involved in chloroplast development, but whether they participate in  
42 photomorphogenesis is largely unknown. Here we show that ELONGATED  
43 HYPOCOTYL5 (HY5) binds to GLK and GNC promoters and activates their  
44 expression. HY5 also interacts with GLK proteins. Chlorophyll content in the  
45 de-etiolating seedlings of the *hy5 glk2* and *hy5 gnc* double mutants was lower  
46 than that in the single mutants. It was further found that GLK inhibited hypocotyl  
47 elongation, whereas GNC promoted hypocotyl elongation, and that both could  
48 superimpose on the *hy5* phenotype. Correspondingly, GLK and GNC differentially  
49 regulate the expression of cell elongation genes. DE-ETIOLATED 1 (DET1)  
50 destabilises GLK proteins. The light-grown traits exhibited by etioplast of *det1*  
51 mutant were attenuated in *det1 glk2* double mutant, while similar to *det1* mutant,  
52 photosystem genes were up-regulated to different extent in etiolated seedlings  
53 overexpressing *GLK2* or *GNC*. Our study reveals that GLK and GNC act  
54 downstream of HY5 and likely cooperate with HY5 and DET1 to orchestrate  
55 multiple developmental traits during the light-induced skotomorphogenesis to  
56 photomorphogenesis transition.

57

58 **Introduction**

59 Light serves as an indispensable resource and the essential regulator for plant  
60 growth. In addition to photosynthesis, light also play roles in regulating seed  
61 germination, seedling de-etiolation, organ development, flowering and other  
62 important physiological processes (Jiao et al., 2007). After germination in  
63 darkness, seeds first grow into etiolated seedlings, displaying long hypocotyls with

64 hooked tops and closed cotyledons. These characteristics are called  
65 skotomorphogenesis. Once the etiolated seedlings break through the soil surface  
66 and receive light, hypocotyl elongation is inhibited, cotyledons open, chloroplasts  
67 develop, and photosynthesis begins. This series of processes is referred to as  
68 photomorphogenesis. Skotomorphogenesis and photomorphogenesis together  
69 ensure that etiolated seedlings emerge from the soil and develop into normal  
70 healthy seedlings, and are both a prerequisite for plant growth and development  
71 ([Sullivan and Deng, 2003](#); [Jiao et al., 2007](#)).

72 As a positive regulator of photomorphogenesis, HY5 acts downstream of  
73 photoreceptors, such as cryptochromes, phytochromes and UV RESISTANCE  
74 LOCUS8 (UVR8), and plays important roles in seedling de-etiolation ([Jiao et al.,](#)  
75 [2007](#); [Stracke et al., 2010](#)). Studies have shown that over 3000 genes can be  
76 directly regulated by the basic leucine zipper (bZIP) transcription factor HY5  
77 ([Jakoby et al., 2002](#); [Lee et al., 2007](#); [Zhang et al., 2011](#)). It regulates many basic  
78 plant growth and development processes, including cell elongation, cell  
79 proliferation, chloroplast development, pigment accumulation, and nutrient uptake  
80 ([Oyama et al., 1997](#); [Shin et al., 2007](#); [Jing et al., 2013](#)). HY5 binds to promoters  
81 through G-box elements and inhibits the expression of cell elongation genes, such  
82 that *hy5* mutants show a typical long hypocotyl phenotype ([Jing et al., 2013](#); [Xu et](#)  
83 [al., 2016b](#)). HY5 is important for chlorophyll and carotenoid accumulation under  
84 light as it regulates the expression of key enzymes such as PHYTOENE  
85 SYNTHASE (PSY) and PROTOCHLOROPHYLLIDE OXIDOREDUCTASE C  
86 (PORC). It also regulates the expression of photosynthetic pigment proteins, such  
87 as light-harvesting chlorophyll-protein complex I subunit A4 (LHCA4)  
88 ([Toledo-Ortiz et al., 2014](#)). HY5 functions through many different regulatory  
89 interactions. For example, it interacts with HY5-HOMOLOGY (HYH) or  
90 CALMODULIN7 (CAM7) protein to binds to the HY5 promoter and activate its own

91 expression (Kushwaha et al., 2008; Abbas et al., 2014; Binkert et al., 2014). The  
92 interaction between HY5 and B-box-containing (BBX) protein BBX21-BBX22  
93 enhances the promoting effect of HY5 on photomorphogenesis, whereas the  
94 interaction between HY5 and BBX24-BBX25 does the opposite, suggesting that  
95 BBX protein acts as coregulator of HY5, for fine-tuning of photomorphogenesis  
96 (Datta et al., 2007; Datta et al., 2008; Xu et al., 2016a). Furthermore, HY5  
97 interacts with PIF1 and PIF3 proteins to coordinate the production of reactive  
98 oxygen species and the temperature control of photosynthetic gene expression  
99 (Chen et al., 2013; Toledo-ortiz et al., 2014). In the case of excess HY5 protein, it  
100 can activate the expression of COP1, thus inducing the degradation of HY5  
101 protein and maintaining it at a relatively stable level (Huang et al., 2012).

102 GOLDEN2 (G2)-LIKE (GLK) and GATA NITRATE-INDUCIBLE CARBON  
103 METABOLISM-INVOLVED (GNC) are two types of transcription factors directly  
104 involved in the regulation of chloroplast development. GLK transcription factors  
105 belong to the GARP superfamily (Fitter et al., 2002), which consists of GLK  
106 (initially from maize), Arabidopsis RESPONSE REGULATOR-B (ARR-B) and  
107 PHOSPHATE STARVATION RESPONSE 1 (PSR1) from Chlamydomonas (Hall et  
108 al., 1998; Imamura et al., 1999; Wykoff et al., 1999). GLKs were first found to  
109 regulate chloroplast development in maize, with a pair of GLK homologs ZmG2  
110 and ZmGLK1 expressed in bundle sheath and mesophyll cells respectively (Hall  
111 et al., 1998; Rossini et al., 2001). In Arabidopsis, GLK1 and GLK2 are regulated  
112 by light, and function redundantly in regulating chlorophyll biosynthesis and  
113 chloroplast development. The leaves and siliques of the double mutant are pale  
114 green, and thylakoid development in the chloroplasts is retarded (Fitter et al.,  
115 2002). Overexpression of GLK1 or GLK2 in *glk1 glk2* double mutants can restore  
116 the defect in chloroplast development (Waters et al., 2008). Ectopic expression of  
117 GLKs was also able to induce increased chloroplast numbers in non-green

118 tissues such as roots and callus of *Arabidopsis* and rice (Nakamura et al., 2009;  
119 Kobayashi et al., 2012a), and in tomato fruits (Nguyen et al., 2014). GLK target  
120 genes are mainly related to chlorophyll biosynthesis, light-harvesting, and  
121 electron transport (Waters et al., 2009; Kobayashi et al., 2012b). In the process of  
122 seedling de-etiolation, GLKs interact with and are phosphorylated by  
123 BRASSINOSTEROID INSENSITIVE2 (BIN2) protein, which promotes the stability  
124 and transcriptional activity of GLK1 (Zhang et al., 2021). GLK also interacts with  
125 ORESARA 1 (ORE1) protein during senescence, with ORE1 antagonizing GLK  
126 induction of target genes (Rauf et al., 2013). The degradation of GLK protein itself  
127 is related to ubiquitination, with GLK2 shown to interact with DET1 protein in  
128 tomato prior to processing by CUL4-DDB1 ubiquitin E3 ligase for degradation  
129 (Tang et al., 2016).

130 The *GATA NITRATE-INDUCIBLE CARBON-METABOLISM-INVOLVED*  
131 (GNC) gene was identified by screening mutants on nitrogen-deficient medium,  
132 with *gnc* mutants accumulating lower chlorophyll than wild type (Bi et al., 2005).  
133 The *CYTOKININ-RESPONSIVE GATA FACTOR1* (CGA1) gene is strongly  
134 induced by cytokinin, and CGA1 is involved in the cytokinin signaling (Naito et al.,  
135 2007). The *gnc cga1* double mutant exhibits decreased chlorophyll content and  
136 decreased chloroplast number. Overexpression of GNC or CGA1 in *Arabidopsis*  
137 resulted in obvious chloroplast development in seedling roots and hypocotyls, and  
138 increased chloroplast number in cotyledon and leaf epidermal cells (Chiang et al.,  
139 2012). Overexpression of CGA1 in rice increases chloroplast number as well as  
140 starch biosynthesis in the leaves (Hudson et al., 2013; Lee et al., 2021). In spite of  
141 the well-known downstream targets of GLK and GNC, their upstream regulation,  
142 particularly in the context of light signaling is not clear. As HY5 is a regulatory hub  
143 in light signaling, and it has been reported that GLK and GNC are dependent on  
144 HY5 in regulating root greening (Kobayashi et al., 2012a, 2017), the molecular

145 relationships between HY5, GLK, and GNC during seedling development are in  
146 need of systematic analysis. It is also important to consider the role of the  
147 COP/DET/FUS complex in regulating GLK and GNC stabilities. DET1 is involved  
148 in the ubiquitination and degradation of positive regulators of  
149 photomorphogenesis in darkness. Apart from shorter hypocotyls and opened  
150 cotyledons, the dark-germinated *det1* mutant seedlings show part of the  
151 light-grown traits, such as expression of photosynthetic genes and development  
152 of thylakoid membranes (Chory et al., 1989). The molecular mechanism behind  
153 such phenotypes in the dark is not fully understood and the potential involvement  
154 of GLK or GNC is worth considering.

155 Therefore, this study focused on the molecular and functional linkages  
156 among HY5, GLK, and GNC/CGA1 transcription factors, aiming to analyze and  
157 clarify the local regulatory network connecting them, so as to better understand  
158 the relationships between light signaling, seedling formation, and chloroplast  
159 development during photomorphogenesis. At the same time, relationships  
160 between GLK, GNC, and DET1, and their effects on the expression of  
161 photosynthetic genes in etiolated seedlings were examined. The results shed light  
162 on the concerted involvement of HY5, GLK, and GNC/CGA1 transcription factors  
163 in both skotomorphogenesis and photomorphogenesis.

164

## 165 **Results**

### 166 **HY5, GLK1/2, and GNC/CGA1 regulate chlorophyll content to different 167 extents in de-etiolating *Arabidopsis* seedlings**

168 HY5, GLKs, and GNC/CGA1 have been reported to regulate the expression of  
169 chlorophyll biosynthesis and photosynthesis related genes (Fitter et al., 2002; Lee  
170 et al., 2007; Waters et al., 2009; Chiang et al., 2012; Hudson et al., 2013;  
171 Toledo-ortiz et al., 2014). To explore the significance of these regulations during

172 photomorphogenesis, we performed systematic investigation in de-etiolating  
173 seedlings. All plants were grown in darkness for 4 days, and then sampled at  
174 different time points in white light to determine chlorophyll content. It was found  
175 that the chlorophyll content in *glk1* mutant had no or little difference from the wild  
176 type, while it was significantly lower in *glk2* mutant, and it decreased more  
177 significantly in *glk1 glk2* double mutant (**Figures 1A and 1C; Supplemental**  
178 **Figures S1A and S1C**). This indicates that both GLKs affect chlorophyll  
179 biosynthesis in seedling de-etiolation process and GLK2 may play a dominant role.  
180 Overexpression of GLK1 or GLK2 in double mutants can compensate for the  
181 phenotype of decreased chlorophyll (**Supplemental Figures S1A and S1C**). The  
182 chlorophyll content of *cga1* mutants was not notably different from the wild type,  
183 while it was lower in *gnc* and *gnc cga1* double mutants, but the difference was  
184 much smaller than that between *glk2* related mutants and the wild type (**Figures**  
185 **1B and 1D; Supplemental Figures S1B and S1D**). The chlorophyll content of  
186 35S:GNC overexpressed material was significantly higher than that of the wild  
187 type in the greening process, while it showed no difference in 35S:CGA1  
188 overexpressed material from that of the wild type at this stage (**Supplemental**  
189 **Figures S1B and S1D**). The chlorophyll content of *hy5* mutant was lower than  
190 that of the wild type, and overexpression of HY5 in the mutant could effectively  
191 compensate for the phenotype (**Figure 1; Supplemental Figure S1**). We  
192 checked the expression of *GLK1*, *GLK2*, *GNC*, and *CGA1* genes in the  
193 de-etiolation process of wild type seedlings, and found that the expression levels  
194 of *GLK2* and *GNC* were more prominent in response to light (**Figure 1E**),  
195 demonstrating again the relative greater importance of them to seedling greening.  
196  
197 **Loss of GLK1/2 or GNC/CGA1 function combined with HY5 mutation has**  
198 **limited further effects on seedling greening**

199 In order to elucidate the genetic relationships between HY5, GLKs and  
200 GNC/CGA1, we constructed double and triple mutants, and investigated the  
201 chlorophyll content in seedlings during de-etiolation. It was found that the  
202 chlorophyll content of *hy5 glk1* double mutant was not different from that of the  
203 wild type and *glk1*. We noticed that the *glk1* single mutant used was caused by an  
204 insertion in the promoter region, and thus the phenotypes in *glk1* single mutant  
205 and *hy5 glk1* double mutant may not be representative of null alleles. On the other  
206 hand, the chlorophyll content of *hy5 glk2* double mutant was lower than that of  
207 *glk2* or *hy5* mutant at 12 h during greening. However, there was no difference in  
208 chlorophyll content between *hy5 glk1 glk2* triple mutant and *glk1 glk2* double  
209 mutant during de-etiolation (**Figures 1A and 1C**). The chlorophyll content in *hy5*  
210 *gnc* and *hy5 cga1* mutants showed little or no difference compared to *hy5*, and  
211 only *hy5 gnc cga1* triple mutant exhibited notably lower chlorophyll content at 12 h  
212 during greening. Moreover, the chlorophyll content of these mutants was generally  
213 higher than that of the *glk* related double or triple mutants (**Figures 1B and 1D**).

214 In order to clarify the chlorophyll phenotype of *hy5* and *glk2* mutants, we  
215 verified the expression levels of some chlorophyll biosynthesis and photosystem  
216 genes in de-etiolating seedlings. At 12 h of light exposure, the expression levels of  
217 chlorophyll biosynthesis genes (*HEMA1*, *PORB*, *PORC* and *CAO*) in *hy5*, *glk2*  
218 and *hy5 glk2* mutants were all remarkably lower than those in the wild type. The  
219 decrease in *glk2* and *hy5 glk2* mutants was not lower than that in the *hy5* mutant,  
220 except for *PORB* (**Figure 2A**). The expression levels of photosystem light  
221 harvesting genes (*LHCB1.2*, *LHCB2.2*, *LHCA1* and *LHCA4*) was also significantly  
222 lower in *hy5*, *glk2*, and *hy5 glk2* mutants than in the wild type, with their  
223 expression in *hy5* mutant considerably higher than those in *glk2* and *hy5 glk2*  
224 mutants (**Figure 2B**). These results indicate that during de-etiolation of seedlings  
225 GLK2 has stronger regulation on photosystem light harvesting genes than HY5,

226 whereas their regulation on chlorophyll biosynthesis may be comparable.

227 To further complement the observed phenotype, we moved on to analyse the  
228 seedlings grown under continuous white light for 4 days, and found similar  
229 differences of chlorophyll content to that during de-etiolation. However, the  
230 chlorophyll content in *hy5 glk1 glk2* triple mutant was lower than that in *glk1 glk2*  
231 double mutant (**Figures 2C and 2D**). We investigated the chloroplast  
232 development in wild type, *glk1 glk2*, *hy5*, and *hy5 glk1 glk2* mutants under  
233 continuous light exposure. Transmission electron microscopy showed that the  
234 chloroplast size of *glk1 glk2* and *hy5 glk1 glk2* mutants was smaller than that of  
235 the wild type and *hy5* mutant, the accumulation of starch grains was decreased,  
236 and the thylakoid stacking was sparser. Even worse, *hy5 glk1 glk2* triple mutant  
237 showed obvious fractured stromal thylakoids (**Figure 2E**), suggesting that *HY5*  
238 mutation combined with *GLK1* and *GLK2* double mutations can lead to further  
239 defects in chloroplast development.

240

#### 241 **HY5 directly regulates *GLK1*, *GLK2*, *GNC* and *CGA1* gene expression**

242 As an extension of the results shown in **Figure 1E**, we found that the expression  
243 levels of *GLK1*, *GLK2*, *GNC* and *CGA1* genes in *hy5* mutants were significantly  
244 lower than those in the wild type (**Figures 1F**), indicating that *HY5* positively  
245 regulates their expression. Typical *cis*-elements to which *HY5* binds to regulate  
246 target gene expression include G-box (CACGTG), T/G-box (CACGTT), E-box  
247 (CAATTG), ACE-Box (ACGT), and Z-Box (ATACGGT) (Shin et al., 2007; Chang et  
248 al., 2008; Catala et al., 2011; Abbas et al., 2014). We performed promoter  
249 analysis for *GLK1* and *GLK2*, and found that their promoter regions contained  
250 *HY5*-binding *cis*-elements. These regions were synthesized to conduct  
251 electrophoretic mobility shift assays (EMSA). It was shown that *HY5* could bind to  
252 *GLK1* and *GLK2* promoter sequences, competitive probes weakened such

253 binding, while the binding ability of mutant probes was much lower than that of  
254 normal probes (**Figure 3A**). In parallel, by transforming protoplasts dual-luciferase  
255 assay displayed that HY5 could activate *GLK1* and *GLK2* expression (**Figures 3B**  
256 **and 3C**). While obtaining the above *in vitro* results, we also validated the binding  
257 *in vivo* via chromatin immunoprecipitation (ChIP) coupled with quantitative PCR  
258 (qPCR) assay. Three or two regions containing HY5 binding elements were  
259 selected from the promoters of *GLK1* and *GLK2* respectively, and the results  
260 demonstrated that the P2 region from *GLK1* promoter and the P1 region from  
261 *GLK2* promoter were most strongly bound by HY5 (**Figure 3D**). *In vitro*  
262 experiment EMSA and dual-luciferase assays confirmed that HY5 could also bind  
263 to *GNC* and *CGA1* promoters to activate their transcription, again followed by *in*  
264 *vivo* experiment ChIP-qPCR showing that the highest enrichment of P1 on *GNC*  
265 and *CGA1* promoters by HY5 (**Figure 3**). In conclusion, HY5 directly binds to the  
266 promoters of *GLK1*, *GLK2*, *GNC*, and *CGA1* to activate their gene expression.

267

### 268 **GLK1/2 and GNC/CGA1 oppositely regulate hypocotyl elongation of 269 light-grown seedlings**

270 HY5 is known to inhibit hypocotyl elongation during photomorphogenesis, as *hy5*  
271 seedlings exhibit longer hypocotyls ([Sullivan and Deng, 2003](#); [Jiao et al., 2007](#)).  
272 Since we found that HY5 directly regulates the expression of *GLK*, *GNC*, and  
273 *CGA1* genes, whether *GLK*, *GNC* and *CGA1* also play roles in seedling  
274 morphological development upon light regulation became the next question.  
275 Therefore, we systematically investigated the hypocotyl phenotypes of a series of  
276 *glk*, *gnc*, and *cga1* mutants. The hypocotyl length of *glk* mutants was measured  
277 under different light quality, and those in *glk1*, *glk2* and *glk1 glk2* mutants were  
278 longer than in wild type, while shorter than in *hy5* mutant, after germinating and  
279 growing under white, blue or red light for 4 days (**Figures 4A and 4B**). When

280 *GLK1* or *GLK2* were overexpressed in *glk1 glk2* mutants, the hypocotyl length  
281 was restored to the level of wild type. There was no significant difference in  
282 hypocotyl length between the mutants and wild type after germinating and  
283 growing for 4 days in darkness (**Supplemental Figure S3**). Together the above  
284 results indicate that GLK inhibits hypocotyl elongation during light-induced  
285 seedling development.

286 We further investigated the hypocotyl phenotype in *hy5* and *glk* double and  
287 triple mutants. Under white or blue light, compared with *hy5*, hypocotyls of *hy5*  
288 *glk1* were slightly longer, while hypocotyls of *hy5 glk2* and *hy5 glk1 glk2* were  
289 significantly longer than that of *hy5*. The hypocotyls of all materials were generally  
290 longer under red light, and those of *hy5 glk1*, *hy5 glk2* and *hy5 glk1 glk2* were still  
291 longer than those of *hy5*, but with smaller differences. No notable differences in  
292 hypocotyl length were observed in dark-grown seedlings between wild type and  
293 these mutants (**Figures 4A and 4B**). We measured the cell length of wild type,  
294 *glk1 glk2*, *hy5*, and *hy5 glk1 glk2* materials in the middle segment of hypocotyls  
295 growing under white light for 4 days, and found that the hypocotyl cell length of  
296 *glk1 glk2* mutant was longer than that of the wild type, and that of *hy5 glk1 glk2*  
297 mutant was longer than that of *hy5* mutant (**Figures 4C and 4D**). In general, there  
298 is an obvious trend of *hy5* < *hy5 glk1* < *hy5 glk2* < *hy5 glk1 glk2* in hypocotyl  
299 length, and GLKs may work independent (at least partly) of HY5 to inhibit  
300 hypocotyl elongation, with GLK2 playing a more important role than GLK1.

301 Different from the hypocotyl phenotype of *glk* series mutants, after  
302 germinating and growing under white light for 4 days, the hypocotyl length of *gnc*,  
303 *cga1* and *gnc cga1* mutants was shorter than that of the wild type, while the  
304 hypocotyl length of 35S:GNC and 35S:CGA1 overexpressed materials was longer  
305 than that of the wild type. There was no difference in hypocotyl length between  
306 these mutants and wild type after germinating and growing in darkness

307 **(Supplemental Figure S4)**, indicating that GNC and CGA1 promoted hypocotyl  
308 elongation under white light. In addition, the hypocotyl length of *hy5 gnc*, *hy5 cga1*  
309 and *hy5 gnc cga1* mutants was shorter than that of *hy5* under white light, but  
310 significantly longer than that of *gnc*, *cga1* and *gnc cga1* mutants (**Figures 4E and**  
311 **4F**), indicating that GNC and CGA1 were able to reduce the inhibition of HY5 on  
312 hypocotyl elongation.

313

314 **Transcriptome and RT-qPCR analysis reveals differential regulation of cell**  
315 **elongation genes by HY5, GLK2, and GNC**

316 The above results showed that the phenotype of *hy5 glk2* mutant was more  
317 severe than that of the *hy5 glk1* mutant, both in regulating chlorophyll content and  
318 inhibiting hypocotyl elongation. Hence, we selected wild type, *glk2*, *hy5*, and *hy5*  
319 *glk2* seedlings that germinated and grew for 4 days under white light for  
320 transcriptome sequencing. As shown in a Venn diagram, *glk2*, *hy5*, and *hy5 glk2*  
321 mutants jointly affected the expression of 142 genes, including 138  
322 down-regulated genes and only 2 up-regulated genes (**Figure 5A**). Deletion of  
323 *HY5* or *GLK2* in most cases resulted in down-regulation of genes, and K-means  
324 clustering showed the same trend (**Figure 5B**), in line with the expectation of  
325 them as positive regulators of photomorphogenesis. Most up-regulated genes  
326 were expressed in *hy5* and *hy5 glk2* mutants. Among the down-regulated genes,  
327 385 were down-regulated together in *hy5* and *hy5 glk2* mutants, while 201 were  
328 down-regulated together in *glk2* and *hy5 glk2* mutants. This is consistent with  
329 *HY5*'s upstream position in activating *GLK* gene expression mentioned above.  
330 The remaining 91 down-regulated genes only in *hy5 glk2* mutants may represent  
331 targets of combined *HY5* and *GLK* activity (**Figure 5A**). According to the trend of  
332 *glk2* < *hy5* < *hy5 glk2* in hypocotyl length, K4 and K7 groups from K-means  
333 clustering could be considered for investigating *GLK2* and *HY5* regulated

334 hypocotyl elongation (**Figure 5B**). In addition, heat map was generated from  
335 differential expression of a list of known cell elongation genes, and a series of  
336 up-regulated genes were considered for subsequent validation (**Figure 5C**).

337 Several elongation genes from **Figure 5C** were selected for RT-qPCR  
338 verification. Among the expression levels of *EXPA5*, *IAA19*, *SAUR20*, and *PME16*,  
339 most of them expressed higher in *glk2* than in wild type, and higher in *hy5* than in  
340 *glk2*. They were detected higher in *hy5 glk2* than in *hy5*, with more variable  
341 degrees (**Figure 5D**). We hypothesized that the interaction between GLK2 and  
342 HY5 proteins could enhance the inhibitory effect on these elongation genes, and  
343 GLK2 may independently inhibit some elongation genes. We also analysed the  
344 expression levels of selected elongation genes in *gnc* and *hy5 gnc* materials. The  
345 expression level of *IAA7* in *gnc* mutant was lower than that in wild type, and the  
346 expression levels of several other genes in *gnc* mutant tended to be lower than in  
347 wild type, although not significant (**Figure 5E**). In addition, the expression levels of  
348 *IAA7*, *IAA19*, *XTH4*, and *PME16* appeared lower in the *hy5 gnc* double mutant  
349 than in *hy5* mutant (**Figure 5E**). These results indicate that GNC could promote  
350 the expression of these elongation genes to less and varying degrees, both  
351 independently or on top of HY5. The primarily targeted hypocotyl elongation  
352 genes by GNC/CGA1 may be largely different from those by GLKs.

353

### 354 **Interaction of HY5 and GLK proteins**

355 Apart from directly targeting many genes to promote their expression, HY5  
356 also interacts with other proteins, HYH or HFR1 for instance, to mutually enhance  
357 protein stability, or together bind to HY5 or downstream gene promoters (Lee et al.,  
358 2007; Ciolfi et al., 2013; Jang et al., 2013). The interaction between HY5 and  
359 G-box binding factor 1 (GBF1) attenuates the activation of *RBCS-1A* by HY5.  
360 Since HY5 interacts with GBF1, and GBF1 interacts with GLK (Tamai et al., 2002;

361 Singh et al., 2012; Ram et al., 2014), we then examined the possibility of HY5  
362 interacting with GLK proteins. In pull-down experiments, the experimental group  
363 GST-GLK1 and GST-GLK2 could pull down HY5 protein, while the control group  
364 could not (**Figure 6A**), indicating that HY5 binds to GLK1 and GLK2. Through  
365 bimolecular luminescence complementation assays, it was found that luciferase  
366 signal could be detected when HY5 was co-transfected with GLK1 and GLK2  
367 proteins, while the signal was not present in the negative controls (**Figure 6B**),  
368 indicating that HY5 interacts with GLK1 and GLK2. The above experiments  
369 provide *in vitro* evidence of HY5 and GLK interaction. We then performed  
370 co-immunoprecipitation assays to confirm that GLK2 interacts with HY5 *in vivo*.  
371 GLK2 fusion protein was immunoprecipitated with FLAG beads, then HY5 fusion  
372 protein was co-precipitated, and was detected by anti-GFP antibody (**Figure 6C**).  
373 HY5 might first activate the expression of *GLK*, and then interacts with GLK  
374 protein to regulate common targets. It should be also pointed out that extra factors  
375 might exist to coordinate the effects of HY5 and GLK2 on their target genes.

376

377 **GLK2 content affects the plastid ultrastructure and photosystem gene  
378 expression in dark-grown *det1* mutant of *Arabidopsis***

379 Compared to the traits of photomorphogenesis, the morphology and gene  
380 expression changes of skotomorphogenesis are relatively less addressed by  
381 previous researches. One of the few but well known observations is that, the  
382 stromal thylakoid membrane was found sufficiently extended in the plastids of  
383 etiolated *det1* mutant seedlings rather than the default form of prolamella body,  
384 and some photosynthetic genes were already expressed in the dark (Chory et al.,  
385 1989). On account of the emphasis on GLK2 from above, we constructed *det1*  
386 *glk2* double mutant and comparative observations were made on the plastid  
387 ultrastructure in the cotyledons of dark-grown *det1*, *glk2*, and *det1 glk2* mutants.

388 As expected, the cotyledons were open in the etiolated *det1 glk2* mutant, and  
389 paler in the light-grown *det1 glk2* mutant (**Figure 7A**). We found that the thylakoid  
390 lamellae in the plastids of *det1 glk2* mutant were less developed than in *det1*  
391 mutant in the dark, although in both cases there was little evidence of a  
392 prolamellar body, indicating that the developed chloroplasts in etiolated *det1*  
393 mutant were related to GLK2 function. By contrast, there was no significant  
394 structural difference of the prolamellar body in *glk2* mutant and  
395 *GLK2*-overexpressing line compared with the wild type, but the size was smaller  
396 or larger respectively (**Figure 7B**).

397 It is known that in the dark, HY5 ubiquitination and degradation are mediated  
398 by the COP/DET/FUS complex (Saijo et al., 2003). In order to study the stability of  
399 GLK proteins in Arabidopsis, we examined the dark-grown wild type and *det1*  
400 mutant using Arabidopsis GLK1 and GLK2 antibodies for Western-blots. The  
401 results showed that both GLK1 and GLK2 protein contents in *det1* mutant were  
402 higher than those in the wild type (**Figure 8A**), suggesting that DET1 may  
403 promote the degradation of GLK proteins. It should be noted that Rubisco large  
404 subunit (RbcL) content was higher in *det1* than in the wild type, which is  
405 consistent with the increased accumulation of *RbcL* transcript in dark-grown *det1*  
406 mutant (Chory et al., 1989). After MG132 (a proteasome inhibitor) treatment, the  
407 accumulation of GLK proteins in the wild type was higher than that in the DMSO  
408 control group, but still much lower than that in the *det1* mutant (**Figure 8A**). The  
409 deficiency of DET1 likely blocked the upstream steps of protein degradation such  
410 as ubiquitination, so that the significant accumulation of GLK proteins in *det1*  
411 mutant was less affected by MG132. Supportively, *in vitro* protein binding  
412 experiments indicate that DET1 interacts with both GLK1 and GLK2 proteins  
413 (**Supplemental Figure S8A**), and GNC and CGA1 proteins as well  
414 (**Supplemental Figure S8B**).

415 The expression of photosynthetic genes in dark-grown *det1* mutant seedlings  
416 is interesting (Chory et al., 1989), but the mechanism of these genes being turned  
417 off in skotomorphogenesis, has not been elucidated. We measured the  
418 expression of photosystem genes in a group of dark-grown *det1* and *g/k2* related  
419 mutants, and found that the expression levels of *LHCB1.2* and *LHCA1* were much  
420 higher in *det1* mutant, but were lower in *g/k2* mutant than those in wild type. The  
421 down-regulation of these genes by GLK2 was also found in *det1 g/k2* double  
422 mutant comparing with the *det1* mutant (Figure 8B). This indicates that GLK2  
423 contributes significantly to the expression of photosystem genes in dark-grown  
424 seedlings, and the effects could be additive to the loss of DET1 function. In the  
425 etiolated materials overexpressing *GLK1*, *GLK2*, *GNC* or *CGA1*, the expression of  
426 *LHCB1.2* and *LHCA1* genes were significantly promoted in *GLK1* or *GLK2*  
427 overexpression lines, less promoted in the *GNC* overexpression line, and least  
428 changed in the *CGA1* overexpression line (Figure 8C). When grown this same set  
429 of materials in the light, increased expression of *LHCB1.2* and *LHCA1* genes were  
430 still observed to larger extent in *GLK1* or *GLK2* overexpression lines than in *GNC*  
431 and *CGA1* overexpression lines relative to the wild type (Figure 8D). Notably,  
432 expression levels of *LHCB1.2* and *LHCA1* genes also increased in both dark and  
433 light-grown *HY5* overexpression lines, but were not higher than those in *GLK1* or  
434 *GLK2* overexpression lines, indicating again that GLKs function at least partly  
435 independent of *HY5* during seedling photomorphogenesis.

436

437 **Discussion**

438 In this work, we have constructed a series of mutant materials to systematically  
439 study the regulatory relationships between *HY5*, *GLK*, and *GNC/CGA1*  
440 transcription factors, as well as their stabilities and functions within the scenario of  
441 skotomorphogenesis and photomorphogenesis. We find that: (1) *HY5* directly

442 activates *GLK*, *GNC*, and *CGA1* expression, and together they positively regulate  
443 chlorophyll biosynthesis and photosystem formation; (2) *GLK* proteins inhibit  
444 hypocotyl elongation, whereas *GNC* and *CGA1* promote hypocotyl elongation, by  
445 differentially regulating the expression of cell elongation genes; (3) In the dark,  
446 *DET1* destabilises *GLK* proteins, and the abnormal light-grown traits exhibited in  
447 the etioplast of *det1* mutant seedlings can be attributed to *GLK2* activity; (4) *GLK2*  
448 maybe the predominant regulator of photosynthetic genes, during both  
449 skotomorphogenesis and photomorphogenesis. At present, the molecular  
450 mechanism of *GLK* and *GNC* in regulating hypocotyl elongation is not entirely  
451 clear. These need to be further investigated in combination with specific genetic  
452 material construction. In addition, *GLK2* function has been standing out in multiple  
453 ways, partially recruited by and interact with *HY5*, and effectively compensates for  
454 *HY5* function, so that it deserves targeted studies in order to guide the potential  
455 application of *GLK2* and *HY5* in crop enhancement.

456

457 **GLK and GNC function downstream but partially independent of HY5 in**  
458 **seedling greening**

459 *HY5* and *GLK* both functions in regulating chlorophyll biosynthesis and chloroplast  
460 development, but targeted studies and clear conclusions are missing on whether  
461 or how the two are related. Studies have shown that  
462 **PHYTOCHROME-INTERACTING FACTOR 4 (PIF4)** in *Arabidopsis* binds to the  
463 promoters of *GLK1* and *GLK2* to inhibit their expression ([Song et al., 2014](#)), while  
464 *HY5* antagonises PIFs to regulate the biosynthesis of photosynthetic pigments  
465 ([Tolede-Ortiz et al., 2014](#)). Besides, microarray studies showed that both  
466 phytochrome A and phytochrome B regulate *GLK* transcription ([Tepperman et al.,](#)  
467 [2006](#)). Considering that *HY5* acts downstream of the photoreceptors, and is a  
468 high-level regulator (many *HY5* targets are other transcription factors) of

469 photomorphogenesis (Lee et al., 2007), there may be a direct positive regulation  
470 of HY5 to *GLKs*. We provided experimental evidences in this work that HY5  
471 indeed binds to the promoters of *GLK* genes and activates their expression.  
472 Similarly, the HY5 regulation of *GNC* and *CGA1* was also confirmed (**Figure 3**).

473 We have constructed double and triple mutants of HY5, GLK1/2, and  
474 GNC/CGA1 to study their functional relationships. Only limited decrease of  
475 chlorophyll content and related gene expression were observed when *hy5 glk2*  
476 mutant was compared to *glk2* mutant, or *hy5 glk1 glk2* mutant was compared to  
477 *glk1 glk2* mutant (**Figures 1 and 2**). Our transcriptome data indicate that,  
478 compared with HY5, GLK2 tends to positively affect more PSII and PSI related  
479 genes (**Supplemental Figure S7**), which was also supported by the stronger  
480 regulation of GLK2 on light harvesting genes than HY5 (**Figure 2B**). When  
481 overexpressing *GLK2* in the *hy5* mutant, the chlorophyll level increased  
482 significantly, although it was still lower than overexpressing *GLK2* in wild type (Liu  
483 et al., 2021). Our study clarifies the downstream relationship of GLKs to HY5, and  
484 implies that GLKs contributes more intensively than HY5, to *Arabidopsis* seedling  
485 greening.

486 It has been reported that HY5 and GLK2 are involved in the greening of  
487 detached root in *Arabidopsis*, and that the GLK2 regulation of root greening  
488 depends to some extent on the presence of HY5 (Kobayashi et al., 2012a). We  
489 observed that the detached roots could still turn green in the absence of a single  
490 GLK or both GLKs, but not in the absence of HY5 (**Supplemental Figure S5**).  
491 The greening process is promoted by the accumulation of endogenous cytokinin  
492 in detached roots (Kobayashi et al., 2012a). In order to investigate the effect of  
493 HY5 and GLKs on cytokinin regulated leaf greening, we added  
494 6-Benzylaminopurine (6-BA) during seedling greening of *hy5 glk* series mutants.  
495 Results showed that 6-BA treatment could promote the accumulation of

496 chlorophyll during this process, with or without GLKs or HY5 (**Supplemental**  
497 **Figure S6**). These results suggest that GLKs and HY5 play similar roles in  
498 response to cytokinin to promote chlorophyll biosynthesis in leaves, whereas HY5  
499 plays a more significant role in detached roots.

500 GLKs seem to exert stronger regulation than GNC/CGA1 in seedling  
501 greening, as *glk* series mutants are much paler than *gnc/cga1* series mutants  
502 (**Figure 1; Supplemental Figure S1**). No difference in chlorophyll content  
503 between *glk1 glk2 gnc cga1* quadruple mutant and *glk1 glk2* mutant was found,  
504 and *CGA1* overexpression in *glk1 glk2* mutant could not restore the chlorophyll  
505 content, while overexpression of *GLK1* partially restores the chlorophyll content in  
506 *gnc cga1* mutants ([Bastakis et al., 2018](#)). Zubo et al. suggested that GLK1/GLK2  
507 and GNC/CGA1 play both overlapping and independent roles in regulating  
508 chlorophyll biosynthesis and chloroplast development ([Zubo et al., 2018](#)). We  
509 further propose that GLKs may play more prominent roles than GNC/CGA1,  
510 downstream but partly independent of HY5, to regulate various targets during the  
511 de-etiolation process of photomorphogenesis.

512  
513 **Differential participation of GLK and GNC in HY5 regulated hypocotyl**  
514 **elongation**

515 The inhibition of hypocotyl elongation, opening of cotyledon, and chloroplast  
516 development are continuous and inseparable processes during seedling  
517 photomorphogenesis. Since HY5 inhibits hypocotyl elongation, we were also  
518 curious about the potential GLK and GNC regulation of hypocotyls. It has been  
519 mentioned that *glk1* seedlings displayed longer hypocotyls and less separated  
520 cotyledons ([Martín et al., 2016](#), [Alem et al., 2022](#)). By systematically analysing the  
521 hypocotyl phenotype of mutants and overexpression lines, we certified that both  
522 GLK1 and GLK2 inhibit hypocotyl elongation, with additive effects on the function

523 of HY5 (**Figures 4A and 4B; Supplemental Figure S3**). Transcriptomic  
524 sequencing and RT-qPCR verification showed that GLK2 itself could inhibit the  
525 expression of elongation genes, and different elongation genes exhibited different  
526 regulatory responses to GLK2 and HY5 (**Figure 5E**).

527 We noticed that the expression levels of some elongation genes were  
528 reported lower in *gnc cga1* mutants than in the wild type ([Xu et al., 2017](#)), and the  
529 seedlings of the *quintuple* mutant of GNC, GNL, and B-GATA had shorter  
530 hypocotyl than wild type ([Ranftl et al., 2016](#)). In this work, we have confirmed that,  
531 contrary to GLK's inhibitory effect, GNC and CGA1 promote hypocotyl elongation,  
532 and the mutation of GNC or CGA1 negatively affects the inhibition of hypocotyl  
533 lengths by HY5 (**Figures 4E and 4F; Supplemental Figure S4**). Our results  
534 indicate that GNC could promote the expression of elongation genes to varying  
535 degrees, independently or on top of HY5 (**Figure 5E**). It should be pointed out that  
536 the same elongation gene maybe differentially regulated by HY5, GLKs, or  
537 GNC/CGA1. In addition, the changes of elongation genes in *glk1 glk2*, *gnc cga1*,  
538 *hy5 glk1 glk2*, and *hy5 gnc cga1* mutants are worth exploring, to clarify the  
539 potential redundant or additive effect of them on hypocotyl length.

540

#### 541 **Significance of GLK2 and GNC in the context of skotomorphogenesis to 542 photomorphogenesis transition**

543 Traits of photomorphogenesis are negatively regulated by the COP/DET/FUS  
544 complex in the dark, which mediates the ubiquitination and proteasome  
545 degradation of positive regulators such as HY5, HYH, LAF1, and HFR1  
546 ([Osterlund et al., 2000; Holm et al., 2002; Seo et al., 2003; Yang et al., 2005](#)).  
547 Interestingly, *det1* and *cop1* mutants exhibit some of the characteristics of  
548 photomorphogenesis during skotomorphogenesis, with shorter hypocotyls, open  
549 cotyledons, and expression of photosynthetic genes ([Chory et al., 1989; Deng et](#)

550 al., 1992). These phenotypes should be related to the accumulation of positive  
551 regulators of photomorphogenesis in darkness, but the specific regulators and  
552 their influence on the phenotypes are not clear. It has been reported that  
553 long-term ABA treatment activates the activity of COP1, which then interacts with  
554 GLK1 protein to mediate its ubiquitination and degradation (Tokumaru et al., 2017;  
555 Lee et al., 2021). In this study we further showed that DET1 is responsible for the  
556 protein degradation of both GLK1 and GLK2 in Arabidopsis seedlings (**Figure 8A**).  
557 As for GLK2, we have constructed *det1 glk2* mutant in Arabidopsis to compare  
558 with *det1* mutant during skotomorphogenesis. The overall number of extended  
559 thylakoid lamellae and expression of photosystem genes were found markedly  
560 reduced in *det1 glk2* compared with *det1* mutant (**Figures 7B and 8B**). In fact,  
561 both GLK2 and GLK1 contribute significantly to the expression of photosystem  
562 genes, not only in the light but also in dark-grown seedlings, while GNC and  
563 CGA1 seem to contribute less than GLKs (**Figures 8C and 8D**). Thus, the  
564 appropriate function of GLKs and GNC/CGA1 is regulated at protein level by  
565 DET1 in etiolated seedlings, while upon light HY5 takes the transcriptional control  
566 and at least partly coordinates their functions, in a regulation cascade of light,  
567 HY5, and GLKs or GNC/CGA1.

568

569 We constructed a working model as shown in **Figure 9**. In dark-grown  
570 seedlings, GLKs, GNC, CGA1 and HY5 proteins are subjected to the DET1  
571 mediated degradation. Photosynthetic genes are inactive and plastid inner  
572 membranes stay at prolamellar body status. After exposure to light, DET1 activity  
573 is inhibited and GLK, GNC, CGA1 and HY5 proteins accumulate. HY5 activates  
574 GLK, GNC and CGA1 genes in a light-dependent manner, and likely interact with  
575 their proteins to cooperatively regulate downstream gene expression to promote  
576 photomorphogenesis. GLKs are master regulators of chloroplast development

577 and able to inhibit hypocotyl elongation independent of HY5. GNC and CGA1 are  
578 less dominant in chloroplast development and able to promote hypocotyl  
579 elongation. These could be the compensation for the relatively weak regulation of  
580 HY5 on chloroplast development, and a sensible way to orchestrate light induced  
581 seedling development, by recruiting multitasking yet complementary regulators.  
582 Our study systematically reveals the new function of GLK and GNC regulating  
583 hypocotyl length under light, refines the local network of HY5, GLKs, GNC and  
584 CGA1, and provides new perspective for better understanding the transition  
585 between dark and light-grown seedlings.

586

## 587 **Materials and methods**

### 588 **Plant materials and growth conditions**

589 Arabidopsis mutants used in this study were in the Columbia (Col-0) background.  
590 The *glk1*, *glk2*, *glk1 glk2*, *gnc*, *cga1*, *gnc cga1*, *hy5*, and *det1* mutants ([Chory et al., 1989; Oyama et al., 1997; Fitter et al., 2002; Chiang et al., 2012](#)), as well as  
591 *35S:GLK1 glk1 glk2*, *35S:GLK2 glk1 glk2*, *35S:GNC*, and *35S:CGA1*  
592 overexpression plants ([Waters et al., 2008; Chiang et al., 2012](#)) were described  
593 previously. Other mutants described in this study were created by crossing from  
594 the above materials. Surface-sterilized seeds were sown onto half-strength  
595 Murashige and Skoog (MS) medium, which contained 1% sucrose and 0.8% agar,  
596 and were cold-treated at 4°C in darkness for 3 days to ensure synchronized  
597 germination, followed by growing in dark or light chambers maintained at 22°C.  
598

599

### 600 **Chlorophyll measurements**

601 Total chlorophylls were extracted by homogenizing the seedlings in 80% acetone,  
602 and leaving the solutions at 4°C for overnight incubation. The absorbance was  
603 detected at wavelength OD<sub>652</sub> with a spectrophotometer. Chlorophyll

604 concentration Ca+b was calculated by OD<sub>652</sub>/34.5 (mg/mL), and then converted  
605 according to the fresh weight of the material (Arnon, 1949; Zhao et al., 2016).

606

### 607 **Hypocotyl length measurement**

608 To measure the hypocotyl length of seedlings, seeds were sown on plates and  
609 stratified at 4°C in darkness for 3 d, and then kept in white light for 4 h in order to  
610 induce uniform germination. The seeds were then transferred to white, blue, red  
611 light, or dark conditions and incubated at 22°C for 4 d. The hypocotyl length were  
612 measured using ImageJ software after photographing the seedlings.

613

### 614 **Transmission electron microscopy**

615 Leaf sections of 2 mm size were cut from the seedlings and fixed in 2.5%  
616 glutaraldehyde, with low vacuum applied for 60 min to assist fixation. Post fixation  
617 in osmium tetroxide, embedding in Spurr's resin, and other steps were performed  
618 by the TEM platform in Center for Excellence in Molecular Plant Sciences,  
619 following standard procedures. The ultra-thin sections were imaged at 80 KV with  
620 a Hitachi H-7650 transmission electron microscope.

621

### 622 **Quantitative RT-PCR**

623 Total RNA was extracted from Col-0 and mutant seedlings using an RNAiso Plus  
624 kit (Takara). Complementary DNAs (cDNA) were synthesized from 2 µg of total  
625 RNA using a Prime Script RT Reagent Kit, with a genomic DNA Eraser (Yeasen).  
626 Then, cDNA was subjected to RT-qPCR assays, using the Step One Plus  
627 RT-PCR detection system (Applied Biosystems) and SYBR Green PCR Master  
628 Mix (Yeasen). PCR was performed in triplicate for each sample, and the  
629 expression levels were normalized to that of *ACT7* gene.

630

631 **Immunoblot analysis**

632 Seedlings were homogenized in a protein extraction buffer containing 100 mM  
633 Tris (pH 6.8), 10% Glycerol, 0.5% SDS, 0.1% Triton, 5 mM EDTA, 0.01 M DTT,  
634 and 1 × complete protease inhibitor cocktail (Roche). Equal amount of proteins  
635 were loaded and separated on a 10% SDS-PAGE gel and transferred to  
636 polyvinylidene fluoride membrane. The membrane was blocked with 5% milk and  
637 incubated with primary antibody overnight at 4°C, washed four times with 1 ×  
638 Phosphate Buffered Saline Tween-20 (PBST) for 5 minutes, and incubated with  
639 secondary antibody for 1 h at room temperature. After four washes with PBST for  
640 5 minutes, signal was detected with ECL kit (Millipore).

641

642 **EMSA assay**

643 Synthetic complementary oligonucleotides of *GLK1*, *GLK2*, *GNC*, and *CGA1* (or  
644 mutant probe with HY5 binding motif mutation) were obtained, and probes were  
645 PCR amplified using Cy5-labeled primers. For proteins, the coding sequence of  
646 HY5 was cloned into pCold-TF vector, expressed, and purified with Capturem™  
647 His-Tagged Purification Maxiprep Kit (Takara). The binding reaction was  
648 performed in 20 µL binding buffer (10 mM Tris pH 8.0, 1 mM KCl, 4 mM MgCl<sub>2</sub>,  
649 0.5mM DTT, 5% glycerol, 0.2 mM EDTA, and 0.01% BSA) using 15 nM probes  
650 and 200 ng proteins, and incubated at room temperature for 30 min. The reactions  
651 were resolved by electrophoresis in a 6% (v/v) native polyacrylamide gel at 4°C.  
652 Cy5-labeled DNA in the gel was scanned by an Amersham Typhoon 5  
653 Biomolecular Imager.

654

655 **Dual-luciferase reporter system**

656 Promoter sub-fragments of *GLK1*, *GLK2*, *GNC*, and *CGA1* were cloned into the  
657 pGreenII 0800-LUC vector to drive the firefly luciferase gene. p2GWY7-HY5-YFP

658 was used as the effector construct. *Arabidopsis* mesophyll cell protoplasts were  
659 isolated and transfected as described previously (Yoo et al., 2007). We used a  
660 Dual Luciferase kit (Yeasen) for transient expression analysis to detect reporter  
661 activity. The Renilla luciferase gene, driven by the cauliflower mosaic virus 35S  
662 promoter, was used as an internal control. The ratio of LUC/REN was calculated  
663 as an indicator of the final transcriptional activity.

664

#### 665 **Chromatin immunoprecipitation (ChIP)**

666 The ChIP assay was performed as described by Xu et al. (2016). Chromatin  
667 isolation was performed using Col-0 and *HA-HY5 hy5-215* transgenic seedlings  
668 grown under constant white light for 4 d. The resuspended chromatin was  
669 sonicated at 4°C to 250-500 bp fragments. The sheared chromatin was  
670 immunoprecipitated, washed, and reverse cross linked. About 10% of sonicated  
671 but non-immunoprecipitated chromatin was reverse cross linked and used as an  
672 input DNA control. Monoclonal anti-HA antibody (ab9110, Abcam, 1:100 dilution)  
673 was used for immunoprecipitation. Both immunoprecipitated DNA and input DNA  
674 were analyzed by RT-PCR. The level of binding was calculated as the ratio  
675 between the IP and Input groups.

676

#### 677 ***In vitro* pull-downs**

678 The full-length coding sequences of *GLK1*, *GLK2*, *GNC*, and *CGA1* were cloned  
679 into pGEX-6P-1 vector, and the full-length coding sequences of *HY5* and *nDET1*  
680 (26-87 aa) were cloned into pCold-TF vector. Two mL of transformed bacteria  
681 cultures were grown over night, diluted 1:100 in the next morning, and grown for  
682 another 3 hours at 37°C. When the cells reached logarithmic phase, 0.1 mM IPTG  
683 was added to induce the expression of proteins at 37°C for 4 hours. Then 0.5 mL  
684 of each selected *E. coli* cultures was added in the same tube, re-suspended in

685 lysis buffer (1 × PBS, pH 7.4, 1 × complete protease inhibitor cocktail), and the  
686 cells were broken with a sonicator for 3 times (30 s on and 60 s off) on ice. After  
687 the cell debris were removed by centrifugation at 18000 g for 30 min, 20  $\mu$ L  
688 Glutathione Sepharose 4B was added to the mixture sample and rotated at 4°C  
689 for 6 hours. After 4 washes with PBST buffer (1 × PBS, pH 7.4, 0.1% Triton X-100),  
690 the pellet fraction was boiled in 5 × SDS protein loading buffer, and the input and  
691 pull-down prey proteins were detected by immunoblot using anti-His (M201,  
692 Takara, 1:3000 dilution) and anti-GST (G018, Abcam, 1:3000 dilution) antibodies  
693 respectively.

694

#### 695 **Bi-luminescence complementation (BiLC) assay**

696 GLK or HY5 was fused to the N- or C-terminus of firefly luciferase, and the  
697 constructs were transformed into agrobacterium (*Agrobacterium tumefaciens*)  
698 strain GV3101. Overnight cultures of agrobacteria were collected by  
699 centrifugation at 4000 g for 10 min, re-suspended in MES buffer (10 mM MES, 10  
700 mM MgCl<sub>2</sub>, and 100 mM acetosyringone), mixed with GV3101 colonies  
701 expressing pSoup-P19 to a final OD<sub>600</sub> = 0.5, and incubated at room temperature  
702 for 3 h in the dark before infiltration. The agrobacterium suspension in a 1 mL  
703 syringe (without the metal needle) was carefully press-infiltrated onto healthy  
704 leaves of 3-week-old *N. benthamiana*. The infiltrated plants were returned to  
705 long-day conditions for 3 d. Leaves were infiltrated with luciferin solution and left  
706 for 10 min, before observing luciferase activity by imaging with a CCD camera  
707 (Tanon-5200, BioTanon, China).

708

#### 709 **Co-immunoprecipitations (Co-IPs)**

710 *Arabidopsis* mesophyll cell protoplasts isolated from two-week-old Col-0  
711 plants grown in long-day conditions were used for co-IP experiments. The

712 protoplasts were transfected with a total of 10  $\mu$ g DNA (p2GWY7-YFP,  
713 p2GWY7-HY5-YFP, and 35S-GLK2-2XFLAG-hcf) and incubated overnight. The  
714 transfected samples were spun for 2 min at 100 g, separated from the  
715 supernatant, and then homogenized in binding buffer (25 mM Tris-HCl, pH 7.5, 1%  
716 [v/v] Triton X-100, 150 mM NaCl, 1 mM EDTA, 10% [v/v] glycerol, and 1x protease  
717 inhibitor cocktail [Roche]) by rotating at 4 °C for 1 h. The insoluble material was  
718 removed by centrifugation at 13,000 g for 10 min at 4 °C, and the supernatant was  
719 mixed with 40  $\mu$ L of ANTI-FLAG M2 affinity beads (Sigma-Aldrich). The mixtures  
720 were incubated overnight at 4 °C for 6 h, and the beads were washed three times  
721 with washing buffer (25 mM Tris-HCl, pH 7.5, 0.5% [v/v] Triton X-100, 150 mM  
722 NaCl, 1 mM EDTA, and 10% [v/v] glycerol). We eluted the bound proteins from the  
723 affinity beads with 2x SDS-PAGE sample buffer and analyzed the eluates by  
724 immunoblotting with anti-GFP (SAB4301138, Sigma-Aldrich, USA, 1:1,000  
725 dilution), anti-FLAG (F1804, Sigma-Aldrich, USA, 1:5,000 dilution), and anti-Actin  
726 (LF208, Epizyme Biotech, China, 1:3,000 dilution) antibodies to detect the target  
727 proteins.

728

### 729 **RNA-seq analysis**

730 Total RNA was extracted from 4-d-old Col-0, *glk2*, *hy5*, and *hy5 glk2* seedlings  
731 grown in constant white light (100  $\mu$ mol photons  $m^{-2} s^{-1}$ ). Sequencing libraries  
732 were generated with three independent biological replicates for each material, and  
733 the sequencing was performed using Illumina platform by Biomarker company  
734 (Beijing). Differentially expressed genes (DEGs) were identified using DESeq  
735 (Version1.18.0) ([Anders et al., 2013](#)).

736

### 737 **Accession numbers**

738 Sequence information from this article can be found in The Arabidopsis

739 Information Resource (TAIR) under the following accession numbers: *GLK1*  
740 (*AT2G20570*), *GLK2* (*AT5G44190*), *GNC* (*AT5G56860*), *CGA1* (*AT4G26150*),  
741 *DET1* (*AT4G10180*), *HY5* (*At5G11260*), *ACT7* (*At5G09810*), *HEMA1*  
742 (*AT1G58290*), *PORB* (*AT4G27440*), *PORC* (*AT1G03630*), *CAO* (*AT1G44446*),  
743 *LHCB1.2* (*AT1G29910*), *LHCB2.2* (*AT2G05070*), *LHCA1* (*AT3G54890*), *LHCA4*  
744 (*AT3G47470*), *EXPA5* (*AT3G29030*), *IAA19* (*AT3G15540*), *SAUR20*  
745 (*AT5G18020*), *PME16* (*AT2G43050*), *IAA7* (*AT3G23050*), and *XTH4*  
746 (*AT2G06850*).

747

748 **Supplemental data**

749 [Supplemental Figure S1](#). HY5, GLK, GNC and CGA1 regulate the chlorophyll  
750 biosynthesis.

751 [Supplemental Figure S2](#). Phenotypes of the mutants and overexpression lines  
752 under continuous white light conditions.

753 [Supplemental Figure S3](#). GLK inhibits hypocotyl elongation.

754 [Supplemental Figure S4](#). GNC and CGA1 promote hypocotyl elongation.

755 [Supplemental Figure S5](#). HY5 but not GLKs is crucial for the greening of detached  
756 roots.

757 [Supplemental Figure S6](#). 6-BA promotes GLK and HY5 dependent chlorophyll  
758 biosynthesis.

759 [Supplemental Figure S7](#). Different expression patterns of HY5 and GLK2  
760 regulated photosystem genes.

761 [Supplemental Figure S8](#). *In vitro* evidence of DET1 interacting with GLK and  
762 GNC/CGA1.

763 [Supplemental Dataset 1](#). List of 516 GLK2 regulated genes.

764 [Supplemental Dataset 2](#). List of 656 HY5 regulated genes.

765 [Supplemental Dataset 3](#). List of 716 HY5 and GLK2 regulated genes.

766 [Supplemental Data 4](#). Primers used in this study.

767 [Supplemental Data 5](#). Statistical analysis for the data shown in figures.

768

769 **Acknowledgments**

770 We thank Prof. Jane Langdale for comments and suggestions on the work. We  
771 thank Xiao-Yan Gao and Zhi-Ping Zhang for technical support on the transmission  
772 electron microscopy. We are grateful to Prof. Hong-Hui Lin for kindly providing the  
773 AtGLK1 antibody; Chun-Guang Chen from ORIZYMES for generating the AtGLK2  
774 antibody; Prof. G. Eric Schaller for gift of Arabidopsis GNC/CGA1 mutants and  
775 overexpression lines.

776

777 **Funding**

778 This work was supported by the National Natural Science Foundation of China  
779 (No. 31970257).

780

781 **References**

782 **Abbas N, Maurya JP, Senapati D, Gangappa SN, and Chattopadhyay S** (2014)  
783      Arabidopsis CAM7 and HY5 physically interact and directly bind to the HY5  
784      promoter to regulate its expression and thereby promote  
785      photomorphogenesis. *Plant Cell* **26**: 1036–1052

786 **Alem AL, Ariel FD, Cho Y, Hong JC, Gonzalez DH, and Viola IL** (2022) TCP15  
787      interacts with GOLDEN2-LIKE 1 to control cotyledon opening in Arabidopsis.  
788      *Plant J* **110(3)**: 748–763

789 **Anders S and Huber W** (2013) Differential expression of RNA-Seq data at the  
790      gene level-the DESeq package. European Molecular Biology Laboratory  
791      (EMBL)

792 **Arnon DI** (1949) Copper enzymes in isolated chloroplasts polyphenoloxidase in  
793      *Bata Vulgaris*. *Plant Physiol* **24**: 1–15

794 **Bastakis E, Hettke B, Klermund C, Grimm B, and Schwechheimer, C** (2018)  
795 LLM-Domain B-GATA transcription factors play multifaceted roles in  
796 controlling greening in *Arabidopsis*. *Plant Cell* **30**: 582–599

797 **Bi YM, Zhang Y, Signorelli T, Zhao R, Zhu T, and Rothstein S** (2005) Genetic  
798 analysis of *Arabidopsis* GATA transcription factor gene family reveals a  
799 nitrate-inducible member important for chlorophyll synthesis and glucose  
800 sensitivity. *Plant J* **44**: 680–692

801 **Binkert M, Kozma-Bognár L, Terecskei K, De Veylder L, Nagy F, and Ulm R**  
802 (2014) UV-B-responsive association of the *Arabidopsis* bZIP transcription  
803 factor *ELONGATED HYPOCOTYL5* with target genes, including its own  
804 promoter. *Plant Cell* **26**: 4200–4213

805 **Catalá R, Medina J, and Salinas J** (2011) Integration of low temperature and  
806 light signaling during cold acclimation response in *Arabidopsis*. *Proc Natl  
807 Acad Sci USA* **108**: 16475–16480

808 **Chang CS, Li YH, Chen LT, Chen WC, Hsieh WP, Shin J, Jane WN, Chou SJ,  
809 Choi G, Hu JM, Somerville S, and Wu SH** (2008) LZF1, a HY5-regulated  
810 transcriptional factor, functions in *Arabidopsis* de-etiolation. *Plant J* **54**: 205–  
811 219

812 **Chen D, Xu G, Tang W, Jing Y, Ji Q, Fei Z, and Lin R** (2013) Antagonistic basic  
813 helix-loop-helix/bZIP transcription factors form transcriptional modules that  
814 integrate light and reactive oxygen species signaling in *Arabidopsis*. *Plant  
815 Cell* **25**: 1657–1673

816 **Chiang YH, Zubro YO, Tapken W, Kim HJ, Lavanway AM, Howard L, Pilon M,  
817 Kieber JJ, and Schaller GE** (2012) Functional characterization of the GATA  
818 transcription factors GNC and CGA1 reveals their key role in chloroplast  
819 development, growth, and division in *Arabidopsis*. *Plant Physiol* **160**: 332–  
820 348

821 **Chory J, Peto C, Feinbaum R, Pratt L, and Ausubel F** (1989) *Arabidopsis*  
822       *thaliana* mutant that develops as a light-grown plant in the absence of light.  
823       *Cell* **58**: 991–999

824 **Ciolfi A, Sessa G, Sassi M, Possenti M, Salvucci S, Carabelli M, Morelli G,**  
825       **and Ruberti I** (2013) Dynamics of the shade-avoidance response in  
826       *Arabidopsis*. *Plant Physiol* **163**: 331–353

827 **Datta S, Hettiarachchi C, Johansson H, and Holm M** (2007) SALT  
828       TOLERANCE HOMOLOG2, a B-box protein in *Arabidopsis* that activates  
829       transcription and positively regulates light-mediated development. *Plant Cell*  
830       **19**: 3242–3255

831 **Datta S, Johansson H, Hettiarachchi C, Irigoyen ML, Desai M, Rubio V, and**  
832       **Holm M** (2008) LZF1/SALT TOLERANCE HOMOLOG3, an *Arabidopsis*  
833       B-box protein involved in light-dependent development and gene expression,  
834       undergoes COP1-mediated ubiquitination. *Plant Cell* **20**: 2324–2338

835 **Deng XW, Matsui M, Wei N, Wagner D, Chu AM, Feldmann KA, and Quail PH**  
836       (1992) COP1, an *Arabidopsis* regulatory gene, encodes a protein with both a  
837       zinc-binding motif and a G beta homologous domain. *Cell* **71**: 791–801

838 **Fitter DW, Martin DJ, Copley MJ, Scotland RW, and Langdale JA** (2002) GLK  
839       gene pairs regulate chloroplast development in diverse plant species. *Plant J*  
840       **31**: 713–727

841 **Hall LN, Rossini L, Cribb L, and Langdale JA** (1998) GOLDEN 2: a novel  
842       transcriptional regulator of cellular differentiation in the maize leaf. *Plant Cell*  
843       **10**: 925–936

844 **Holm M, Ma LG, Qu LJ, and Deng XW** (2002) Two interacting bZIP proteins are  
845       direct targets of COP1-mediated control of light-dependent gene expression  
846       in *Arabidopsis*. *Genes Dev* **16**: 1247–1259

847 **Huang X, Ouyang X, Yang P, Lau OS, Li G, Li J, Chen H, and Deng XW** (2012)

848       Arabidopsis FHY3 and HY5 positively mediate induction of COP1  
849       transcription in response to photomorphogenic UV-B light. *Plant Cell* **24**:  
850       4590–4606

851       **Hudson D, Guevara DR, Hand AJ, Xu Z, Hao L, Chen X, Zhu T, Bi YM, and**  
852       **Rothstein SJ** (2013). Rice cytokinin GATA transcription Factor1 regulates  
853       chloroplast development and plant architecture. *Plant Physiol* **162**: 132–144

854       **Imamura A, Hanaki N, Nakamura A, Suzuki T, Taniguchi M, Kiba T, Ueguchi C,**  
855       **Sugiyama T, and Mizuno T** (1999) Compilation and characterization of  
856       Arabidopsis thaliana response regulators implicated in His-Asp phosphorelay  
857       signal transduction. *Plant Cell Physiol* **40**: 733–742

858       **Jakoby M, Weisshaar B, Dröge-Laser W, Vicente-Carbajosa J, Tiedemann J,**  
859       **Kroj T, Parcy F, and bZIP Research Group** (2002) bZIP transcription factors  
860       in Arabidopsis. *Trends Plant Sci* **7**: 106–111

861       **Jang IC, Henriques R, and Chua NH** (2013) Three transcription factors, HFR1,  
862       LAF1 and HY5, regulate largely independent signaling pathways downstream  
863       of phytochrome A. *Plant Cell Physiol* **54**: 907–916

864       **Jiao Y, Lau OS, and Deng XW** (2007) Light-regulated transcriptional networks in  
865       higher plants. *Nat Rev Genet* **8**: 217–230

866       **Jing Y, Zhang D, Wang X, Tang W, Wang W, Huai J, Xu G, Chen D, Li Y, and**  
867       **Lin R** (2013) Arabidopsis chromatin remodeling factor PICKLE interacts with  
868       transcription factor HY5 to regulate hypocotyl cell elongation. *Plant Cell* **25**:  
869       242–256

870       **Kobayashi K, Baba S, Obayashi T, Sato M, Toyooka K, Keränen M, Aro EM,**  
871       **Fukaki H, Ohta H, Sugimoto K, and Masuda T** (2012a) Regulation of root  
872       greening by light and auxin/cytokinin signaling in Arabidopsis. *Plant Cell* **24**:  
873       1081–1095

874       **Kobayashi K, Obayashi T, and Masuda T** (2012b) Role of the G-box element in

875 regulation of chlorophyll biosynthesis in *Arabidopsis* roots. *Plant Signal*  
876 *Behav* **7**: 922–926

877 **Kobayashi K, Ohnishi A, Sasaki D, Fujii S, Iwase A, Sugimoto K, Masuda T,**  
878 **and Wada H** (2017) Shoot Removal Induces Chloroplast Development in  
879 Roots via Cytokinin Signaling. *Plant Physiol* **173**: 2340–2355

880 **Kushwaha R, Singh A, and Chattopadhyay S** (2008) Calmodulin7 plays an  
881 important role as transcriptional regulator in *Arabidopsis* seedling  
882 development. *Plant Cell* **20**: 1747–1759

883 **Lee D, Hua L, Khoshravesh R, Giuliani R, Kumar I, Cousins A, Sage TL,**  
884 **Hibberd JM, and Brutnell TP** (2021) Engineering chloroplast development  
885 in rice through cell - specific control of endogenous genetic circuits. *Plant*  
886 *Biotechnol J* **19**(11): 2291–2303

887 **Lee J, Choi B, Yun A, Son N, Ahn G, Cha JY, Kim WY, and Hwang I** (2021)  
888 Long-term abscisic acid promotes golden2-like1 degradation through  
889 constitutive photomorphogenic 1 in a light intensity-dependent manner to  
890 suppress chloroplast development. *Plant Cell Environ* **44**: 3034–3048

891 **Lee J, He K, Stolc V, Lee H, Figueroa P, Gao Y, Tongprasit W, Zhao H, Lee I,**  
892 **and Deng XW** (2007) Analysis of transcription factor HY5 genomic binding  
893 sites revealed its hierarchical role in light regulation of development. *Plant*  
894 *Cell* **19**: 731–749

895 **Liu D, Zhao D, Li X, and Zeng YJ** (2022) AtGLK2, an *Arabidopsis*  
896 GOLDEN2-LIKE transcription factor, positively regulates anthocyanin  
897 biosynthesis via AtHY5-mediated light signaling. *Plant Growth Regul* **96**: 79–  
898 90

899 **Martín G, Leivar P, Ludevid D, Tepperman JM, Quail PH, and Monte E** (2016)  
900 Phytochrome and retrograde signalling pathways converge to  
901 antagonistically regulate a light-induced transcriptional network. *Nat*

902 Commun 7: 11431

903 **Naito T, Kiba T, Koizumi N, Yamashino T, and Mizuno T** (2007)

904 Characterization of a unique GATA family gene that responds to both light

905 and cytokinin in *Arabidopsis thaliana*. *Biosci Biotechnol Biochem* **71**: 1557–

906 1560

907 **Nakamura H, Muramatsu M, Hakata M, Ueno O, Nagamura Y, Hirochika H,**

908 **Takano M, and Ichikawa H** (2009) Ectopic overexpression of the

909 transcription factor OsGLK1 induces chloroplast development in non-green

910 rice cells. *Plant Cell Physiol* **50**: 1933–1949

911 **Nguyen CV, Vrebalov JT, Gapper NE, Zheng Y, Zhong S, Fei Z, and**

912 **Giovannoni JJ** (2014) Tomato GOLDEN2-LIKE transcription factors reveal

913 molecular gradients that function during fruit development and ripening. *Plant*

914 *Cell* **26**: 585–601

915 **Osterlund MT, Hardtke CS, Wei N, and Deng XW** (2000) Targeted

916 destabilization of HY5 during light-regulated development of *Arabidopsis*.

917 *Nature* **405**: 462–466

918 **Oyama T, Shimura Y, and Okada K** (1997) The *Arabidopsis* HY5 gene encodes

919 a bZIP protein that regulates stimulus-induced development of root and

920 hypocotyl. *Genes Dev* **11**: 2983–2995

921 **Ram H, Priya P, Jain M, and Chattopadhyay S** (2014) Genome-wide DNA

922 binding of GBF1 is modulated by its heterodimerizing protein partners, HY5

923 and HYH. *Mol Plant* **7**: 448–451

924 **Ranftl QL, Bastakis E, Klermund C, and Schwechheimer C** (2016)

925 LLM-Domain Containing B-GATA Factors Control Different Aspects of

926 Cytokinin-Regulated Development in *Arabidopsis thaliana*. *Plant Physiol*

927 **170(4)**: 2295–2311

928 **Rauf M, Arif M, Dortay H, Matallana-Ramírez LP, Waters MT, Gil Nam H, Lim**

929 **PO, Mueller-Roeber B, and Balazadeh S** (2013) ORE1 balances leaf  
930 senescence against maintenance by antagonizing G2-like-mediated  
931 transcription. *Embo Rep* **14**: 382–388

932 **Rossini L, Cribb L, Martin DJ, and Langdale JA** (2001) The maize golden2  
933 gene defines a novel class of transcriptional regulators in plants. *Plant Cell* **13**:  
934 1231–1244

935 **Saijo Y, Sullivan JA, Wang H, Yang J, Shen Y, Rubio V, Ma L, Hoecker U, and**  
936 **Deng XW** (2003) The COP1-SPA1 interaction defines a critical step in  
937 phytochrome A-mediated regulation of HY5 activity. *Genes Dev* **17**: 2642–  
938 2647

939 **Seo HS, Yang JY, Ishikawa M, Bolle C, Ballesteros ML, and Chua NH** (2003)  
940 LAF1 ubiquitination by COP1 controls photomorphogenesis and is stimulated  
941 by SPA1. *Nature* **423**: 995–999

942 **Shin J, Park E, and Choi G** (2007) PIF3 regulates anthocyanin biosynthesis in  
943 an HY5-dependent manner with both factors directly binding anthocyanin  
944 biosynthetic gene promoters in *Arabidopsis*. *Plant J* **49**: 981–994

945 **Singh A, Ram H, Abbas N, and Chattopadhyay S** (2012) Molecular interactions  
946 of GBF1 with HY5 and HYH proteins during light-mediated seedling  
947 development in *Arabidopsis thaliana*. *J Biol Chem* **287**: 25995–26009

948 **Song Y, Yang C, Gao S, Zhang W, Li L, and Kuai B** (2014) Age-triggered and  
949 dark-induced leaf senescence require the bHLH transcription factors PIF3, 4,  
950 and 5. *Mol Plant* **7**: 1776–1787

951 **Stracke R, Favory JJ, Gruber H, Bartelniewoehner L, Bartels S, Binkert M,**  
952 **Funk M, Weisshaar B, and Ulm R** (2010) The *Arabidopsis* bZIP transcription  
953 factor HY5 regulates expression of the PFG1/MYB12 gene in response to  
954 light and ultraviolet-B radiation. *Plant Cell Environ* **33**: 88–103

955 **Sullivan JA and Deng XW** (2003) From seed to seed: the role of photoreceptors

956 in *Arabidopsis* development. *Dev Biol* **260**: 289–297

957 **Tamai H, Iwabuchi M, and Meshi T** (2002) *Arabidopsis* GARP transcriptional  
958 activators interact with the Pro-rich activation domain shared by  
959 G-box-binding bZIP factors. *Plant Cell Physiol* **43**: 99–107

960 **Tang X, Miao M, Niu X, Zhang D, Cao X, Jin X, Zhu Y, Fan Y, Wang H, Liu Y, Sui Y, Wang W, Wang A, Xiao F, Giovannoni J, and Liu Y** (2016) Ubiquitin-conjugated degradation of golden 2-like transcription factor is  
961 mediated by CUL4-DDB1-based E3 ligase complex in tomato. *New Phytol*  
962 **209**: 1028–1039

963 **Tepperman JM, Hwang Y-S, and Quail PH** (2006) phyA dominates in  
964 transduction of red-light signals to rapidly responding genes at the initiation of  
965 *Arabidopsis* seedling de-etiolation. *Plant J* **48**: 728–742

966 **Tokumaru M, Adachi F, Toda M, Ito-Inaba Y, Yazu F, Hirosawa Y, Sakakibara Y, Suiko M, Kakizaki T, and Inaba T** (2017) Ubiquitin-Proteasome Dependent  
967 Regulation of the GOLDEN2-LIKE 1 Transcription Factor in Response to  
968 Plastid Signals. *Plant Physiol* **173**: 524–535

969 **Toledo-Ortiz G, Johansson H, Lee KP, Bou-Torrent J, Stewart K, Steel G, Rodríguez-Concepción M, and Halliday KJ** (2014) The HY5-PIF regulatory  
970 module coordinates light and temperature control of photosynthetic gene  
971 transcription. *PLoS Genet* **10**: e1004416

972 **Waters MT, Moylan EC, and Langdale JA** (2008) GLK transcription factors  
973 regulate chloroplast development in a cell-autonomous manner. *Plant J* **56**:  
974 432–444

975 **Waters MT, Wang P, Korkaric M, Capper RG, Saunders NJ, and Langdale JA**  
976 (2009) GLK transcription factors coordinate expression of the photosynthetic  
977 apparatus in *Arabidopsis*. *Plant Cell* **21**: 1109–1128

978 **Wykoff DD, Grossman AR, Weeks DP, Usuda H, and Shimogawara K** (1999)

983           Psr1, a nuclear localized protein that regulates phosphorus metabolism in  
984           Chlamydomonas. *Proc Natl Acad Sci USA* **96**: 15336–15341

985   **Xu D, Jiang Y, Li J, Lin F, Holm M, and Deng XW** (2016a) BBX21, an  
986           Arabidopsis B-box protein, directly activates HY5 and is targeted by COP1 for  
987           26S proteasome-mediated degradation. *Proc Natl Acad Sci USA* **113**: 7655–  
988           7660

989   **Xu X, Chi W, Sun X, Feng P, Guo H, Li J, Lin R, Lu C, Wang H, Leister D, and**  
990           **Zhang L** (2016b) Convergence of light and chloroplast signals for  
991           de-etiolation through ABI4-HY5 and COP1. *Nat Plants* **2**: 16066

992   **Xu Z, Casaretto JA, Bi YM, and Rothstein SJ** (2017) Genome-wide binding  
993           analysis of AtGNC and AtCGA1 demonstrates their cross-regulation and  
994           common and specific functions. *Plant Direct* **1**: e00016

995   **Yang J, Lin R, Sullivan J, Hoecker U, Liu B, Xu L, Deng XW, and Wang H**  
996           (2005) Light regulates COP1-mediated degradation of HFR1, a transcription  
997           factor essential for light signaling in Arabidopsis. *Plant Cell* **17**: 804–821

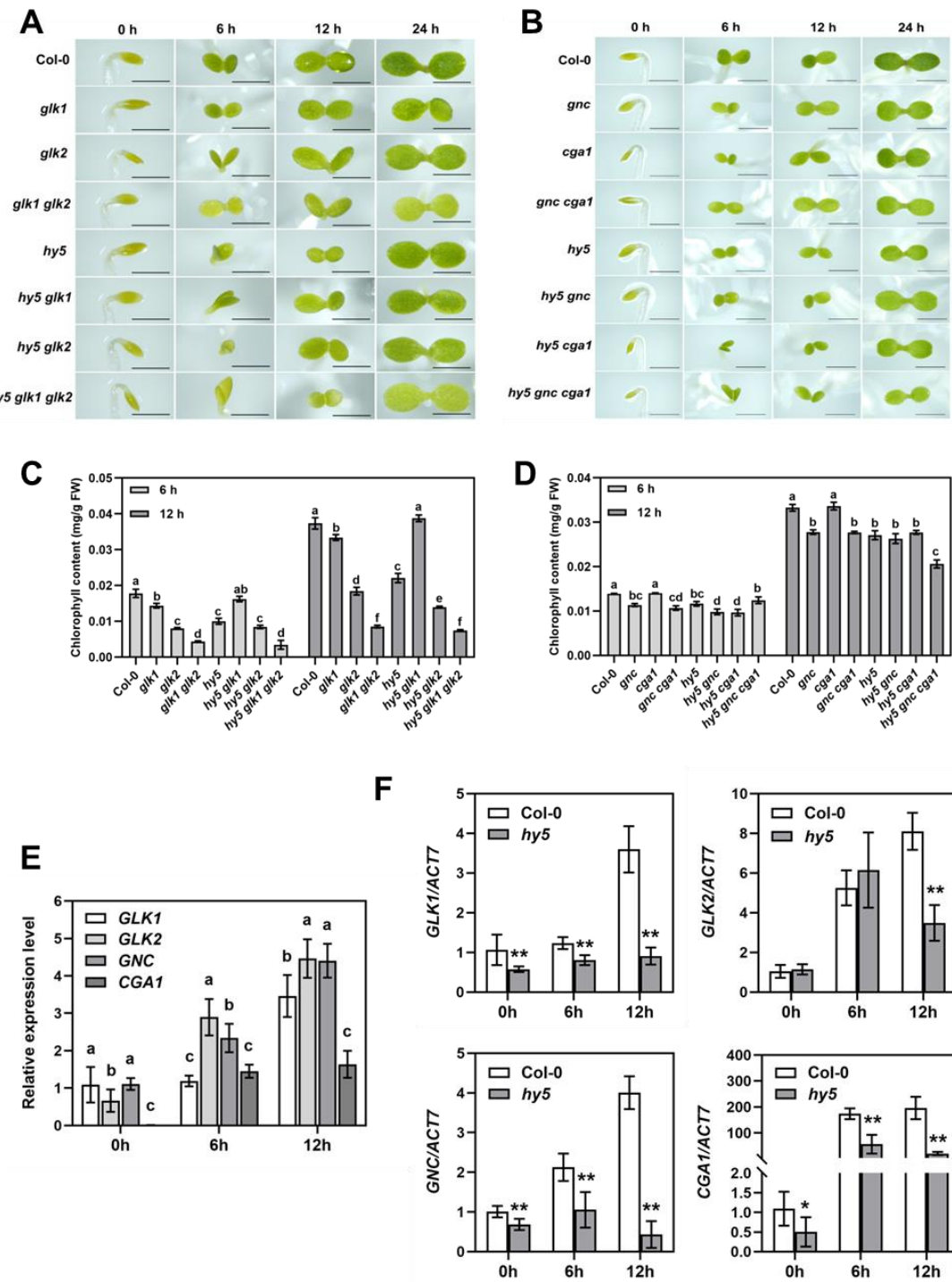
998   **Yoo SD, Cho YH, and Sheen J** (2007) Arabidopsis mesophyll protoplasts: a  
999           versatile cell system for transient gene expression analysis. *Nat Protoc* **2(7)**:  
1000           1565–1572

1001   **Zhang D, Tan W, Yang F, Han Q, Deng X, Guo H, Liu B, Yin Y, and Lin H** (2021)  
1002           A BIN2-GLK1 Signaling Module Integrates Brassinosteroid and Light  
1003           Signaling to Repress Chloroplast Development in the Dark. *Dev Cell* **56**:  
1004           310–324 e317

1005   **Zhang H, He H, Wang X, Wang X, Yang X, Li L, and Deng XW** (2011)  
1006           Genome-wide mapping of the HY5-mediated gene networks in Arabidopsis  
1007           that involve both transcriptional and post-transcriptional regulation. *Plant J* **65**:  
1008           346–358

1009   **Zhao YR, Li X, Yu KQ, Cheng F, and He Y** (2016) Hyperspectral Imaging for

1010 Determining Pigment Contents in Cucumber Leaves in Response to Angular  
1011 Leaf Spot Disease. *Sci Rep* **6**: 27790  
1012 **Zubo YO, Blakley IC, Franco-Zorrilla JM, Yamburenko MV, Solano R, Kieber**  
1013 **JJ, Loraine AE, and Schaller GE** (2018) Coordination of Chloroplast  
1014 Development through the Action of the GNC and GLK Transcription Factor  
1015 Families. *Plant Physiol* **178**: 130–147  
1016  
1017



1018

1019

1020 **Figure 1.** GLK1/2 and GNC/CGA1 positively regulate chlorophyll content  
1021 downstream of HY5 during de-etiolation.

1022

1023 **(A)** Phenotypes of 4-day-old etiolated seedlings of Col-0, *glk1*, *glk2*, *glk1 glk2*, *hy5*,

1024 *hy5 glk1*, *hy5 glk2*, and *hy5 glk1 glk2* during transition from dark to light conditions  
1025 for 6 h, 12 h, 24 h. Scale bars = 1 mm.

1026 **(B)** Phenotypes of 4-day-old etiolated seedlings of Col-0, *gnc*, *cga1*, *gnc cga1*,  
1027 *hy5*, *hy5 gnc*, *hy5 cga1*, and *hy5 gnc cga1* during transition from dark to light  
1028 conditions for 6 h, 12 h, 24 h. Scale bars = 1 mm.

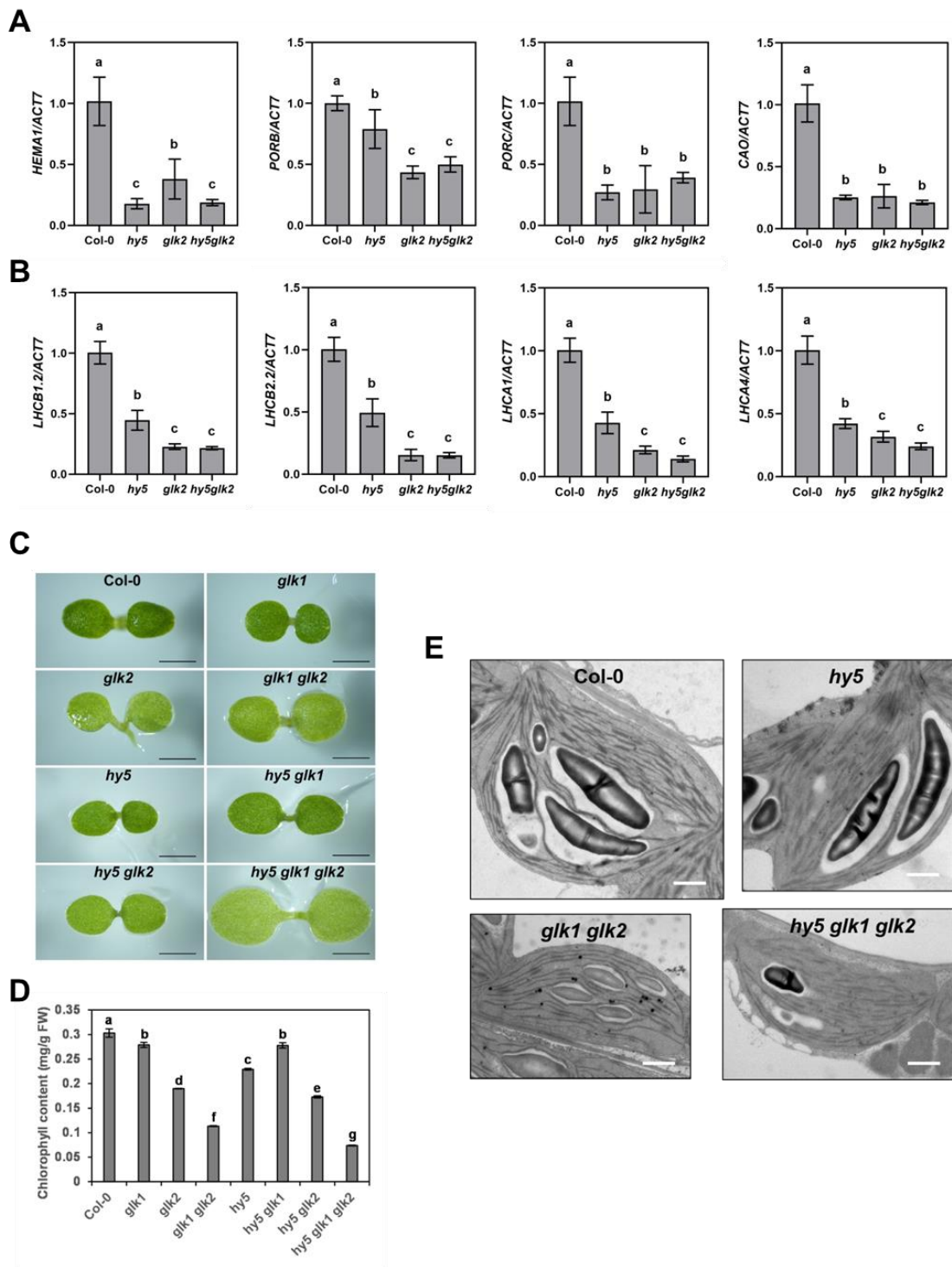
1029 **(C, D)** Chlorophyll contents of de-etiolating seedlings during transition from (A)  
1030 and (B) dark to light for 6 h and 12 h. The data represent means  $\pm$  SD (n = 3) and  
1031 letters above the bars indicate significant differences ( $P < 0.05$ ), as determined by  
1032 one-way ANOVA with Turkey's HSD test.

1033 **(E)** The expression levels of *GLK1*, *GLK2*, *GNC* and *CGA1* in 4-d-old dark-grown  
1034 Col-0 upon being transferred to white light at indicated time points. The *ACT7*  
1035 gene was used as internal control. The data represent means  $\pm$  SD (n = 3) and  
1036 letters above the bars indicate significant differences ( $P < 0.05$ ), as determined by  
1037 one-way ANOVA with Turkey's HSD test.

1038 **(F)** The expression levels of *GLK1*, *GLK2*, *GNC* and *CGA1* in 4-d-old dark-grown  
1039 Col-0 and *hy5* seedlings upon being transferred to white light at indicated time  
1040 points. The data represent means  $\pm$  SD (n = 3), and asterisks indicate a significant  
1041 difference compared with Col-0 (\* $P < 0.05$ , \*\* $P < 0.01$ , paired samples *t*-test).

1042

1043



1044  
1045

1046 **Figure 2.** Chloroplast development and photosynthetic gene expression is further  
1047 impaired in *hy5* and *glk* multiple mutants.

1048

1049 **(A, B)** RT-qPCR analysis of chlorophyll biosynthesis and photosystem genes

1050 expressed in 4-d-old etiolated seedlings of Col-0, *hy5*, *glk2* and *hy5 glk2* upon  
1051 being transferred to white light for 12 h. The *ACT7* gene was used as internal  
1052 control. The data represent means  $\pm$  SD (n = 3) and letters above the bars  
1053 indicate significant differences ( $P < 0.05$ ), as determined by one-way ANOVA with  
1054 Turkey's HSD test.

1055 **(C)** Phenotypes of 4-day-old Col-0, *glk1*, *glk2*, *glk1 glk2*, *hy5*, *hy5 glk1*, *hy5 glk2*,  
1056 and *hy5 glk1 glk2* seedlings grown on half-strength MS plates under continuous  
1057 white light conditions. Scale bars = 1 mm.

1058 **(D)** Chlorophyll contents of the genotypes shown in **(A)**. The data represent  
1059 means  $\pm$  SD (n = 3) and letters above the bars indicate significant differences ( $P <$   
1060 0.05), as determined by one-way ANOVA with Turkey's HSD test.

1061 **(E)** The ultrastructure of mesophyll cell chloroplasts of Col-0, *hy5*, *glk1 glk2*, and  
1062 *hy5 glk1 glk2* seedlings grown under continuous white light for 7 days. Scale bar =  
1063 1  $\mu$ m.

1064

1065

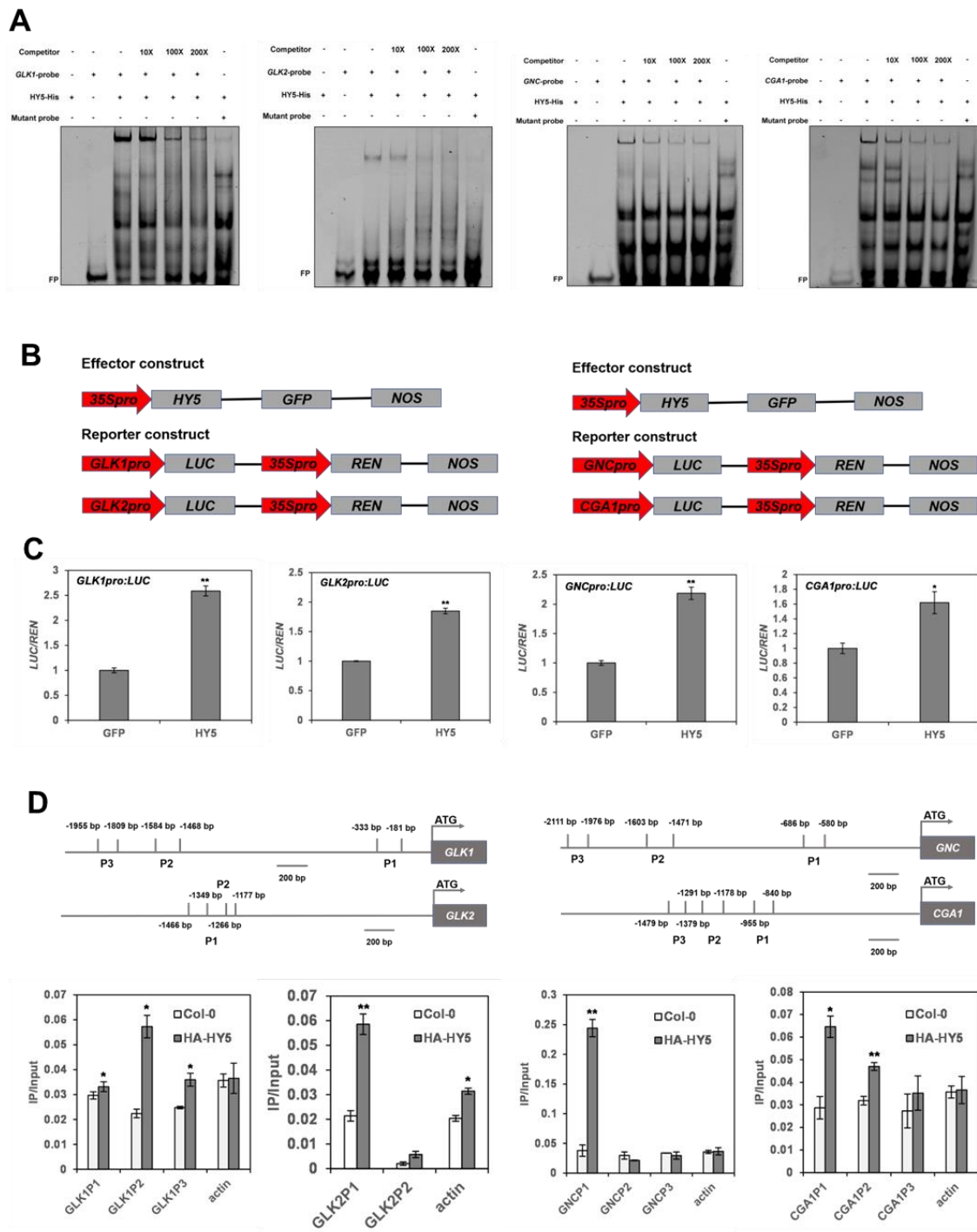
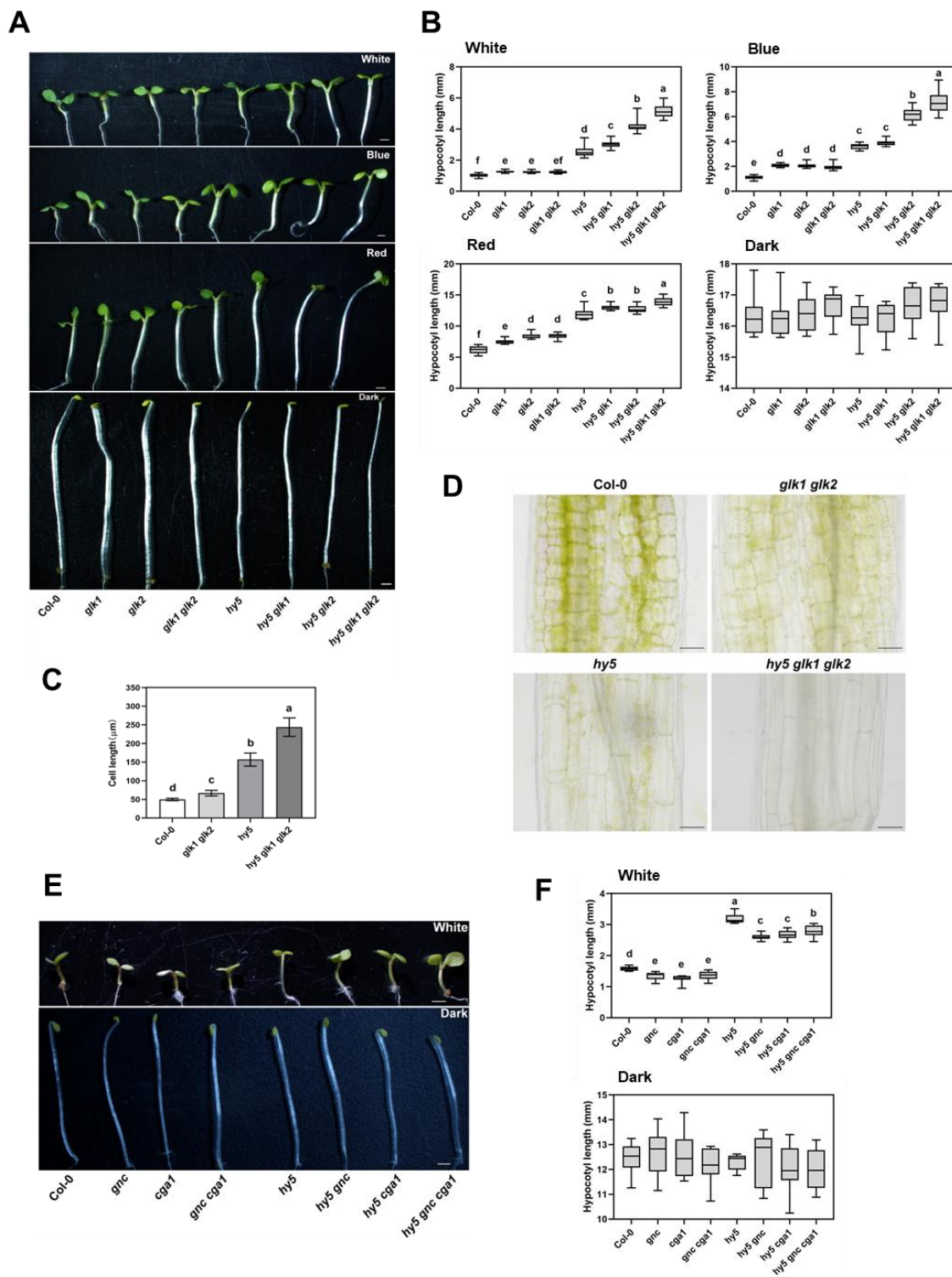


**Figure 3.** Binding of HY5 to the promoters and transcriptional activation of *GLK1*, *GLK2*, *GNC* and *CGA1*.

**(A)** EMSA showing HY5 binds to the sub-fragments of promoters of *GLK1*, *GLK2*, *GNC* and *CGA1* *in vitro*. “-” and “+” indicate the absence and presence of

1073 corresponding probes or proteins. FP means free probe.  
1074 **(B)** Schematic structures of effector and reporter constructs used in  
1075 dual-luciferase (LUC) reporter system. *REN*, renilla luciferase gene.  
1076 **(C)** Bar graphs showing HY5 induces the activation of *GLK1pro:LUC*,  
1077 *GLK2pro:LUC*, *GNCpro:LUC* and *CGA1pro:LUC*. The data represent means  $\pm$  SD  
1078 (n = 4), and asterisks indicate a significant difference compared with control  
1079 (\*P<0.05, \*\*P<0.01, paired samples t-test).  
1080 **(D)** Illustration of *GLK1*, *GLK2*, *GNC* and *CGA1* promoter regions with the  
1081 indicated positions of primers used in ChIP-qPCR. Bar graphs showing  
1082 ChIP-qPCR assays that HY5 associates with the promoters in vivo. Col-0 material  
1083 and *ACTIN* gene were used as negative controls. The data represent means  $\pm$  SD  
1084 (n = 3), and asterisks indicate a significant difference compared with Col-0  
1085 (\*P<0.05, \*\*P<0.01, paired samples t-test).  
1086  
1087



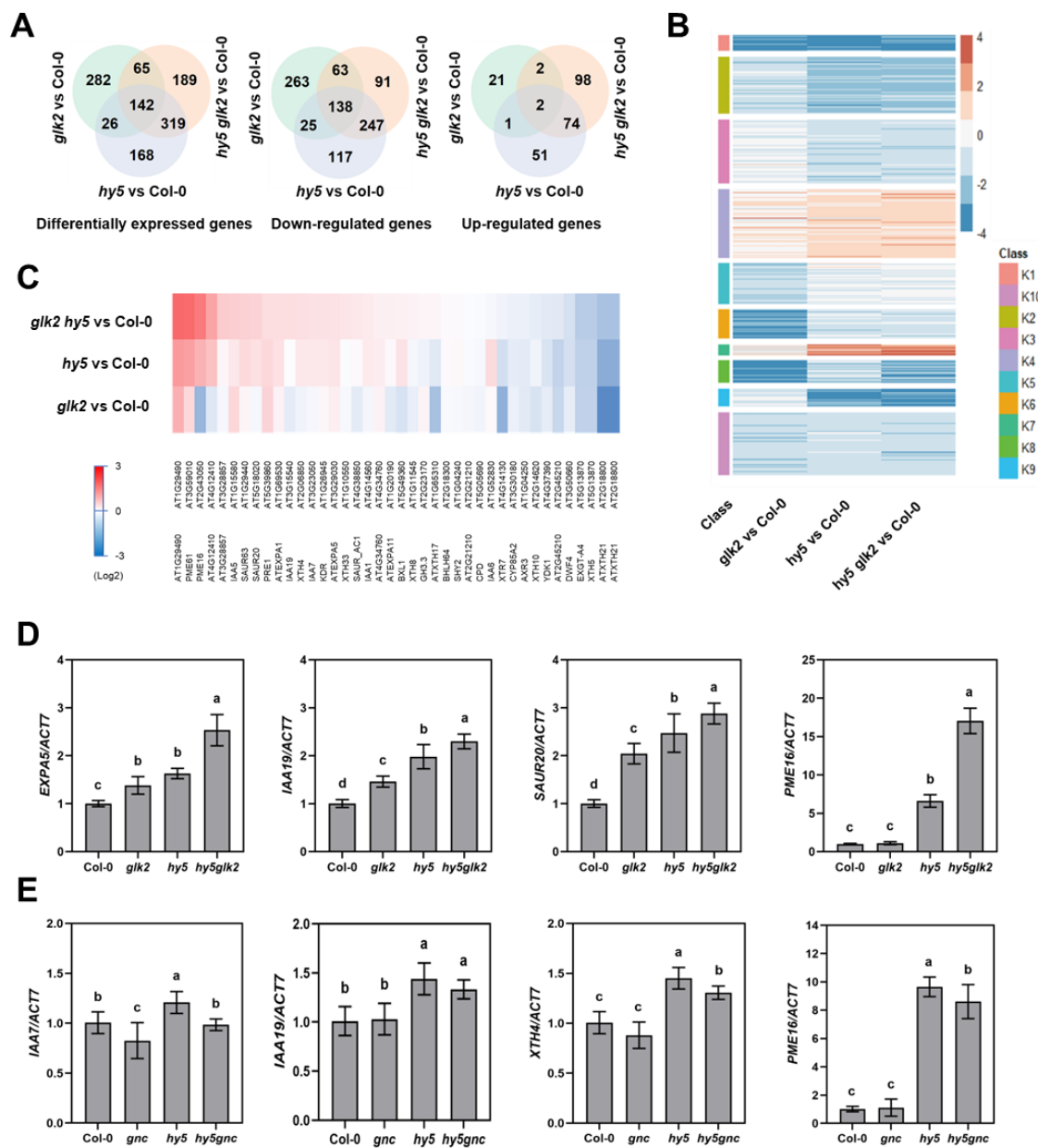
1088

1089

1090 **Figure 4.** GLK1/2 negatively and GNC/CGA1 positively regulate hypocotyl  
1091 elongation.

1092

1093 **(A)** Phenotypes of 4-d-old Col-0, *glk1*, *glk2*, *glk1 glk2*, *hy5*, *hy5 glk1*, *hy5 glk2*, and  
1094 *hy5 glk1 glk2* seedlings grown in white (100  $\mu\text{mol/m}^2/\text{s}$ ), blue (60  $\mu\text{mol/m}^2/\text{s}$ ), red  
1095 (90  $\mu\text{mol/m}^2/\text{s}$ ) light and dark conditions. Scale bar = 1 mm.  
1096 **(B)** Quantification of hypocotyl lengths indicated in (A). The data represent means  
1097  $\pm$  SD (n  $\geq$ 17) and letters above the bars indicate significant differences ( $P < 0.05$ ),  
1098 as determined by one-way ANOVA with Turkey's HSD test.  
1099 **(C)** Quantification of hypocotyl cell length from 4-d-old Col-0, *glk1 glk2*, *hy5*, and  
1100 *hy5 glk1 glk2* seedlings, grown in white light (100  $\mu\text{mol/m}^2/\text{s}$ ) conditions. The data  
1101 represent means  $\pm$  SD (n = 15) and letters above the bars indicate significant  
1102 differences ( $P < 0.05$ ), as determined by one-way ANOVA with Turkey's HSD test.  
1103 **(D)** Hypocotyl cell length phenotypes from 4-d-old Col-0, *glk1 glk2*, *hy5*, and *hy5*  
1104 *glk1 glk2* seedlings. Scale bar = 20  $\mu\text{m}$ .  
1105 **(E)** Phenotypes of 4-d-old Col-0, *gnc*, *cga1*, *gnc cga1*, *hy5*, *hy5 gnc*, *hy5 cga1*,  
1106 and *hy5 gnc cga1* seedlings grown in white light (100  $\mu\text{mol/m}^2/\text{s}$ ) and dark  
1107 conditions. Scale bar = 1 mm.  
1108 **(F)** Quantification of hypocotyl lengths indicated in (E). The data represent means  
1109  $\pm$  SD (n  $\geq$ 15) and letters above the bars indicate significant differences ( $P < 0.05$ ),  
1110 as determined by one-way ANOVA with Turkey's HSD test.  
1111  
1112



1113  
1114

1115 **Figure 5.** Different expression patterns of HY5, GLK2, and GNC regulated  
1116 elongation genes.

1117

1118 **(A)** Venn diagram showing overlaps between sets of differentially expressed  
1119 genes in *glk2*, *hy5* and *hy5 glk2* mutants, relative to Col-0.

1120 **(B)** K-means clustering of differentially expressed genes regulated by GLK2, HY5  
1121 and both. The scale bar shows fold changes (log2 value).

1122 **(C)** Expression patterns of cell elongation genes in *glk2*, *hy5* and *hy5 glk2*  
1123 mutants, relative to Col-0. The scale bar shows fold changes (log2 value). Heat

1124 map was aligned according to fold changes in *hy5 glk2* mutant.  
1125 **(D, E)** RT-qPCR analysis of cell elongation genes expressed in 4-d-old Col-0, *hy5*,  
1126 *glk2*, *hy5 glk2*, *gnc*, and *hy5 gnc* seedlings grown under continuous white light.  
1127 The *ACT7* gene was used as internal control. The data represent means  $\pm$  SD (n  
1128 = 3) and letters above the bars indicate significant differences ( $P < 0.05$ ), as  
1129 determined by one-way ANOVA with Turkey's HSD test.

1130

1131

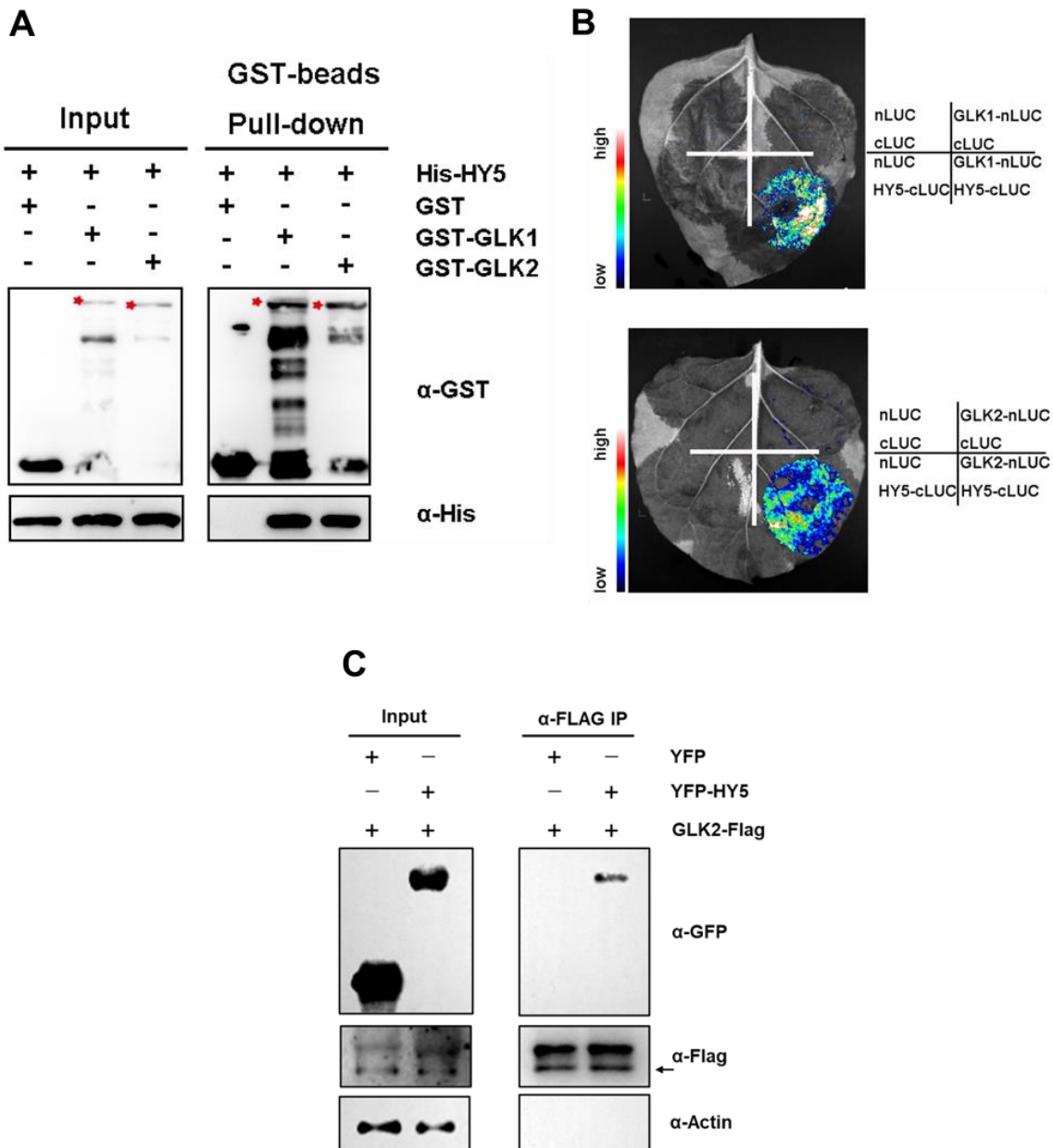
1132

1133

1134

1135

1136



1137

1138

1139 **Figure 6.** Evidences of HY5 interacting with GLK proteins.

1140

1141 **(A)** *In vitro* pulldown assays showing the interaction of GLK1 and GLK2 with HY5.  
 1142 GST-GLK protein or GST protein were used to pull down His-HY5 protein using  
 1143 GST beads. Anti-GST and anti-His antibodies were used for immunoblot analysis.  
 1144 “-” and “+” indicate the absence and presence of corresponding proteins.

1145 **(B)** Bimolecular luminescence complementation assays showing GLK1 and GLK2  
 1146 can interact with HY5. nLUC and cLUC served as negative controls.

1147 **(C)** Co-immunoprecipitation assays using a transient expression system in

1148 Arabidopsis mesophyll cell protoplast, showing that GLK2 interacts with HY5 *in*  
1149 *vivo*. Protein extract was precipitated with FLAG beads, and fusion proteins were  
1150 detected by immunoblot analysis using anti-GFP and anti-FLAG antibodies.

1151

1152

1153

1154

1155

1156

1157

1158

1159

1160

1161

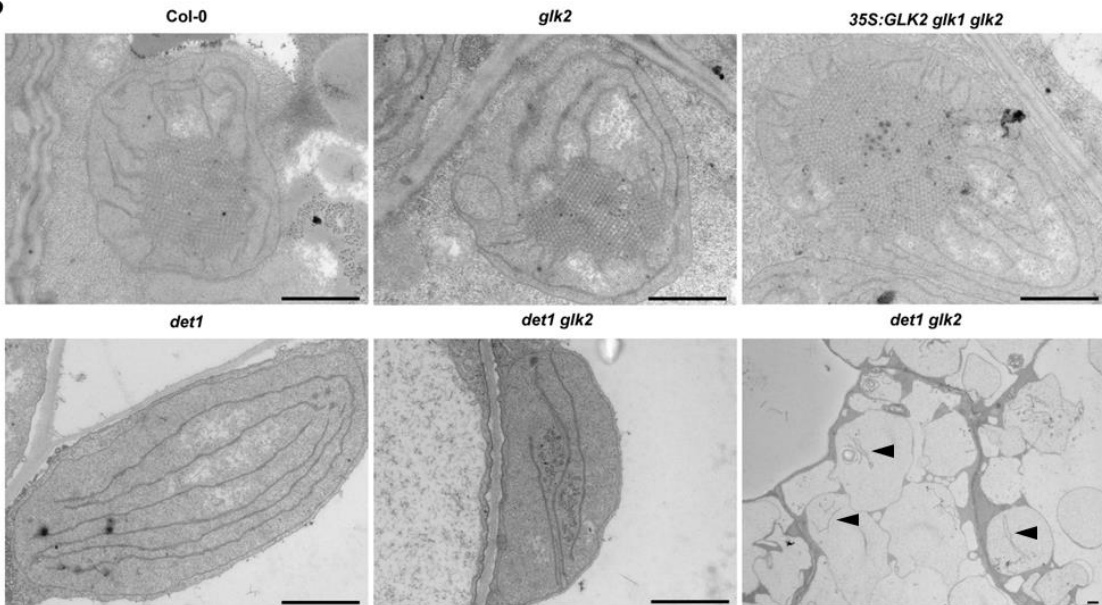
1162

1163

A



B



1164

1165

1166 **Figure 7.** GLK2 is responsible for the developed thylakoid structures in the  
1167 etiolated *det1* mutant.

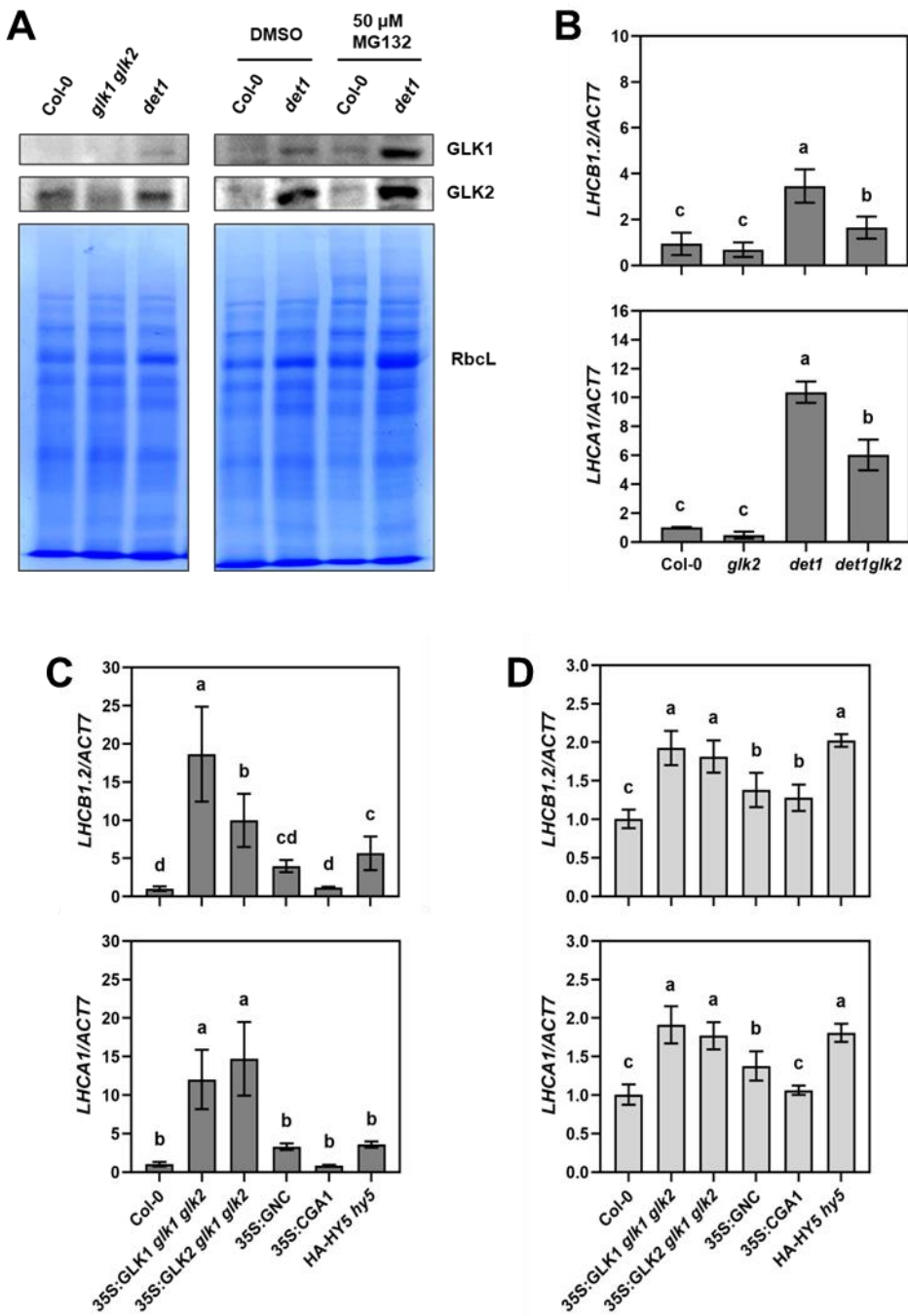
1168

1169 **(A)** Phenotype of 4 d dark (upper panel) or light (lower panel) grown Col-0, *glk2*,  
1170 *det1*, and *det1 glk2* seedlings. Scale bars represent 500  $\mu$ m (upper panel) or 1  
1171 mm (lower panel).

1172 **(B)** The ultrastructure of mesophyll chloroplasts of Col-0, *glk2*, 35S:GLK2 *glk1*  
1173 *glk2*, *det1*, and *det1 glk2* seedlings grown under dark condition for 4 days. Scale  
1174 bar = 1  $\mu$ m. Black arrow heads in the bottom right image point to the thylakoid  
1175 lamellae in very few amount.

1176

1177



1178

1179

1180 **Figure 8.** DET1 promotes the degradation of GLK protein, and GLK is responsible  
1181 for photosystem gene expression in the etiolated *det1* mutant.

1182

1183 **(A)** Immunoblot detection of GLK1 and GLK2 in Col-0, *gik1 gik2*, and *det1*  
1184 seedlings grown in the dark for 4 d (left). GLK protein levels in 4-d-old dark-grown  
1185 Col-0 and *det1* seedlings after 12 h treatment with 50  $\mu$ M MG132 or DMSO (right).

1186 Coomassie stained PAGE gel was shown as loading control, and the band of  
1187 Rubisco large subunit was indicated.

1188 **(B)** RT-qPCR analysis of photosystem genes expressed in 4-d-old etiolated Col-0,  
1189 *glk2*, 35S:*GLK2* *glk1* *glk2*, *det1*, and *det1* *glk2* seedlings.

1190 **(C, D)** RT-qPCR analysis of photosystem genes expressed in 4-d-old etiolated (D)  
1191 or light-grown (E) Col-0, 35S:*GLK1* *glk1* *glk2*, 35S:*GNC*, 35S:*CGA1*, and *HA-HY5*  
1192 *hy5* seedlings. The *ACT7* gene was used as internal control. The data represent  
1193 means  $\pm$  SD (n = 3) and letters above the bars indicate significant differences (P <  
1194 0.05), as determined by one-way ANOVA with Turkey's HSD test.

1195

1196

1197

1198

1199

1200

1201

1202

1203

1204

1205

1206

1207

1208

1209

1210

1211

1212

1213

1214

1215

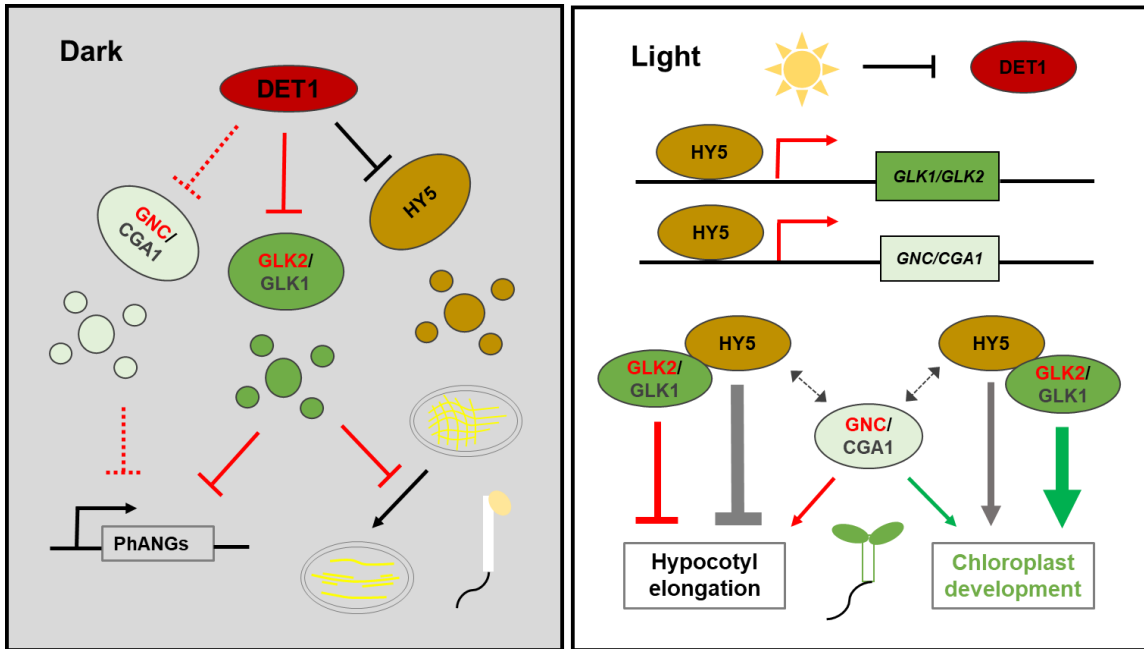
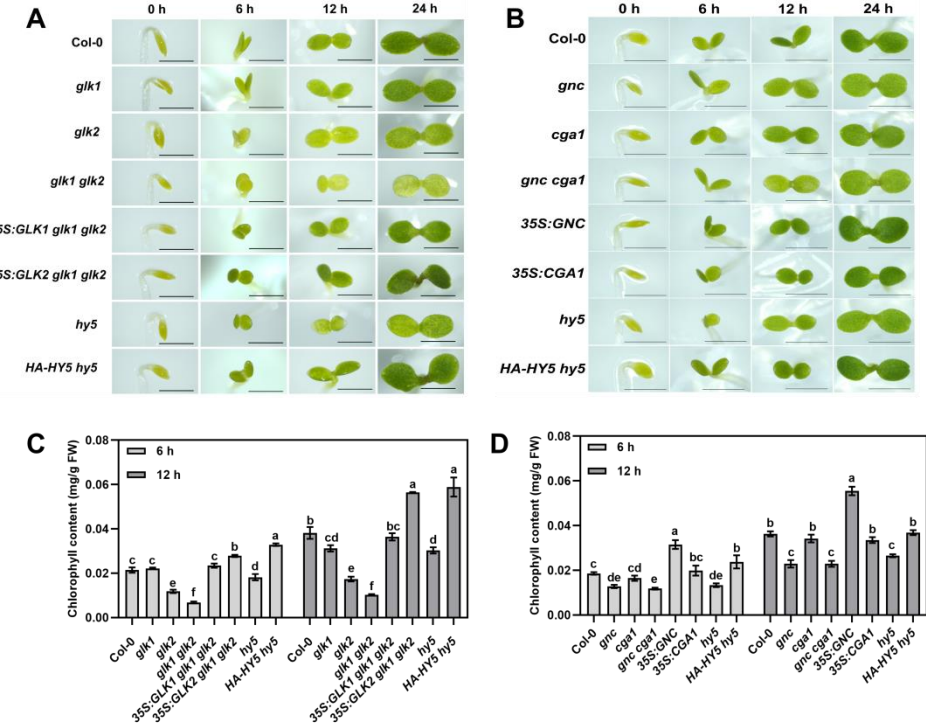


**Figure 9.** A working model depicting GLKs, GNC/CGA1, and HY5 in the regulation of skotomorphogenesis and photomorphogenesis.

GLKs, GNC, CGA1 and HY5 undergo DET1-mediated degradation in the dark, so that the expression of photosynthesis associated nuclear genes (PhANGs), and the transformation of prolamellar body towards extended lamellae are inhibited. Light inhibits DET1 activity, and HY5 directs the promoter of GLKs, GNC and CGA1, inducing their activities to promote chloroplast development. The protein interactions between HY5 and GLKs are shown. GLKs inhibit hypocotyl elongation while GNC and CGA1 promote hypocotyl elongation. Thick green arrow indicates strong promotion of chloroplast development by GLKs. Thick gray line indicates strong inhibition of hypocotyl elongation by HY5. Thinner arrows indicate less strong regulation. Dashed lines in the dark indicate GNC/CGA1 related regulations that pending to be further validated. Dashed double sided arrows in the light indicate potential protein interactions of HY5 with GNC/CGA1.



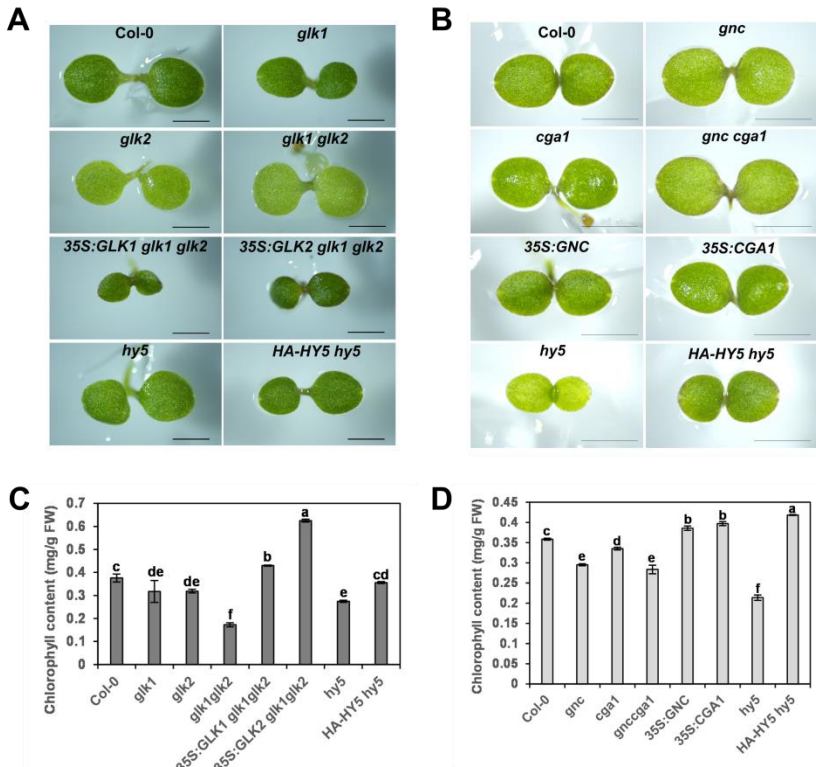
**Supplemental Figure S1.** HY5, GLK, GNC and CGA1 regulate the chlorophyll content. (Supports Figure 1)

**(A)** Representative images of 4-day-old etiolated seedlings of Col-0, *glk1*, *glk2*, *glk1 glk2*, 35S:GLK1 *glk1 glk2*, 35S:GLK2 *glk1 glk2*, *hy5*, and *HA-HY5 hy5* during the transition from dark to light conditions for 6 h, 12 h, and 24 h. Scale bars = 1 mm.

**(B)** Representative images of 4-day-old etiolated seedlings of Col-0, *gnc*, *cga1*, *gnc cga1*, 35S:GNC, 35S:CGA1, *hy5*, and *HA-HY5 hy5* during the transition from dark to light conditions for 6 h, 12 h, and 24 h. Scale bars = 1 mm.

**(C)** Chlorophyll contents of 4-day-old etiolated seedlings from **(A)** during the transition from dark to light conditions for 6 h and 12 h. The data represent means  $\pm$  SD (n=3) and letters above the bars indicate significant differences ( $P < 0.05$ ), as determined by one-way ANOVA with Turkey's HSD test. The experiments were performed three times with similar results.

**(D)** Chlorophyll contents of 4-day-old etiolated seedlings from **(B)** during the transition from dark to light conditions for 6 h and 12 h. The data represent means  $\pm$  SD (n=3) and letters above the bars indicate significant differences ( $P < 0.05$ ), as determined by one-way ANOVA with Turkey's HSD test. The experiments were performed three times with similar results.



1259

1260

**Supplemental Figure S2.** Phenotypes of the mutants and overexpression lines under continuous light conditions. (Supports Figure 2)

1263

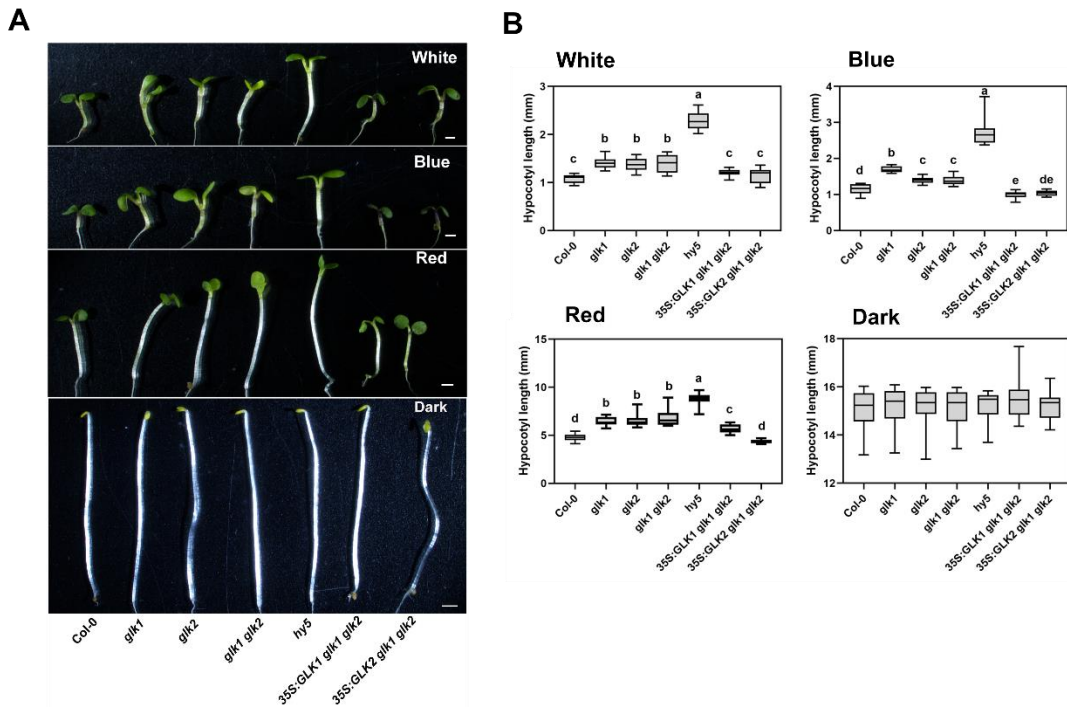
1264 **(A)** Representative images of 4-day-old Col-0, *glk1*, *glk2*, *glk1 glk2*, *35S:GLK1*  
1265 *glk1 glk2*, *35S:GLK2 glk1 glk2*, *hy5*, and *HA-HY5 hy5* seedlings grown on  
1266 half-strength MS plates for 4 days under continuous white light conditions. Scale  
1267 bars = 1 mm.

1268 **(B)** Representative images of 4-day-old Col-0, *gnc*, *cga1*, *gnc cga1*, *35S:GNC*,  
1269 *35S:CGA1*, *hy5*, and *HA-HY5 hy5* seedlings grown on half-strength MS plates for  
1270 4 days under continuous white light conditions. Scale bars = 1 mm.

1271 **(C)** Chlorophyll contents of the genotypes shown in **(A)**. The data represent  
1272 means  $\pm$  SD (n=3) and letters above the bars indicate significant differences (P <  
1273 0.05), as determined by one-way ANOVA with Turkey's HSD test. The  
1274 experiments were performed three times with similar results.

1275 **(D)** Chlorophyll contents of the genotypes shown in **(B)**. The data represent  
1276 means  $\pm$  SD (n=3) and letters above the bars indicate significant differences (P <  
1277 0.05), as determined by one-way ANOVA with Turkey's HSD test. The  
1278 experiments were performed three times with similar results.

1279



1280

1281

1282 **Supplemental Figure S3. GLK inhibits hypocotyl elongation. (Supports Figure 4)**

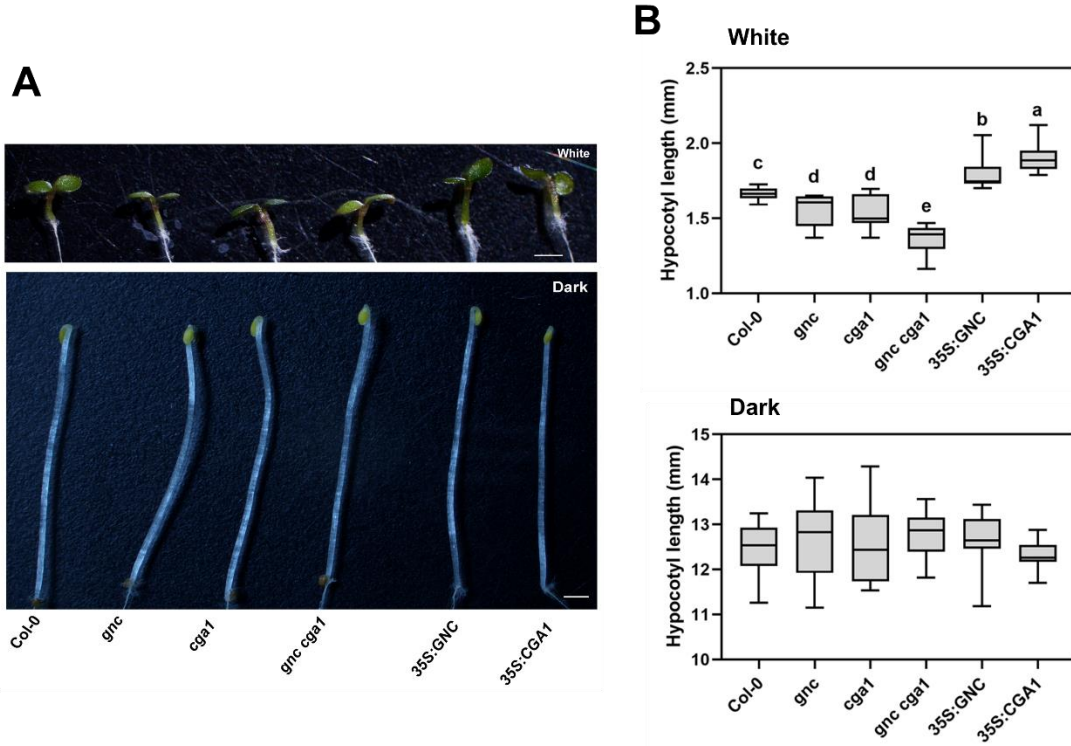
1283

1284 **(A)** Hypocotyl phenotypes of 4-d-old Col-0, *gik1*, *gik2*, *gik1 gik2*, *hy5*, 35S:GLK1  
1285 *gik1 gik2*, and 35S:GLK2 *gik1 gik2* seedlings grown in white (100  $\mu\text{mol}/\text{m}^2/\text{s}$ ), blue  
1286 (60  $\mu\text{mol}/\text{m}^2/\text{s}$ ), red (90  $\mu\text{mol}/\text{m}^2/\text{s}$ ) light and dark conditions. Scale bar = 1 mm.

1287 **(B)** Quantification of hypocotyl lengths indicated in **(A)**. The data represent means  
1288  $\pm$  SD (n  $\geq$ 18) and letters above the bars indicate significant differences ( $P < 0.05$ ),  
1289 as determined by one-way ANOVA with Turkey's HSD test. The experiments were  
1290 performed three times with similar results.

1291

1292



1293

1294

1295 **Supplemental Figure S4.** GNC and CGA1 promote hypocotyl elongation.  
1296 (Supports Figure 4)

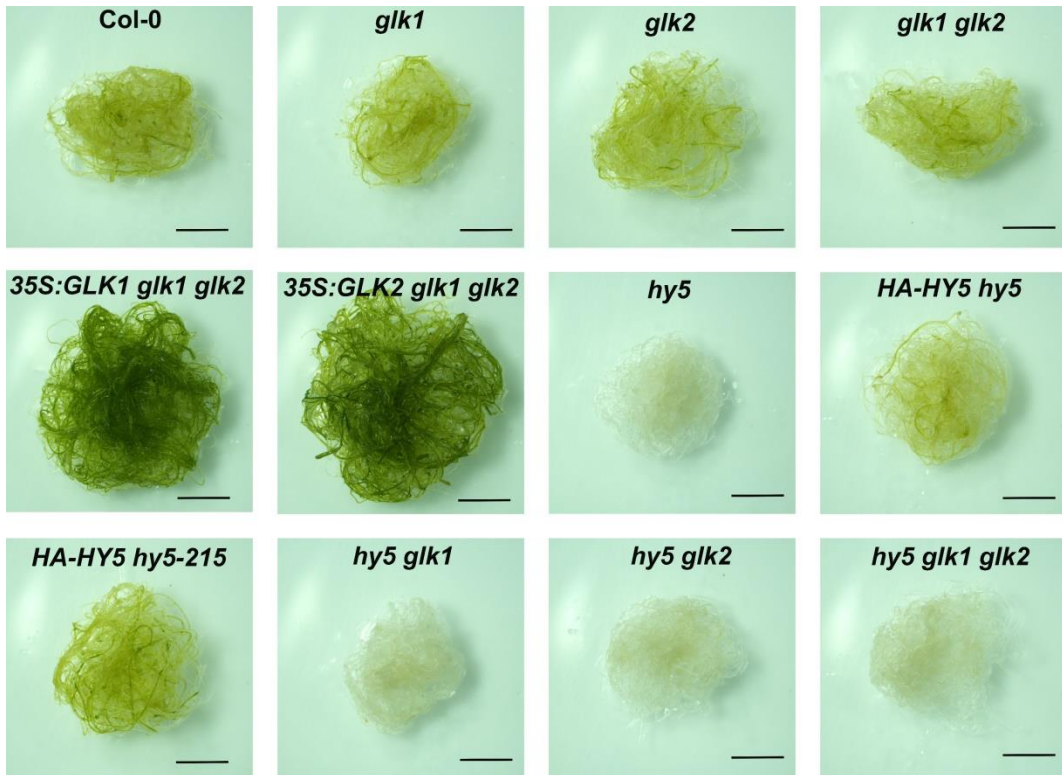
1297

1298 **(A)** Hypocotyl phenotypes of 4-d-old Col-0, gnc, cga1, gnc cga1, 35S:GNC, and  
1299 35S:CGA1 seedlings grown in white light (100  $\mu\text{mol}/\text{m}^2/\text{s}$ ) and dark conditions.  
1300 Scale bar = 1 mm.

1301 **(B)** Quantification of hypocotyl lengths indicated in **(A)**. The data represent means  
1302  $\pm$  SD ( $n \geq 15$ ) and letters above the bars indicate significant differences ( $P < 0.05$ ),  
1303 as determined by one-way ANOVA with Turkey's HSD test. The experiments were  
1304 performed three times with similar results.

1305

1306



1307

1308

1309 **Supplemental Figure S5.** HY5 but not GLKs is crucial for the greening of  
1310 detached roots.

1311

1312 Root samples were detached from 7-d-old seedlings, and then cultured on  
1313 hormone-free MS medium for 14 d. Scale bar = 5 mm.

1314

1315

1316

1317

1318

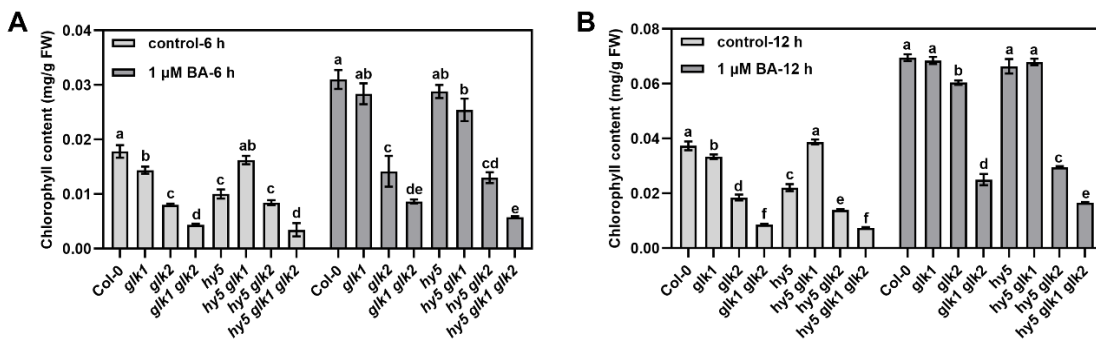
1319

1320

1321

1322

1323



1324

1325

1326 **Supplemental Figure S6.** 6-BA promotes the GLK and HY5 dependent  
1327 chlorophyll content.

1328

1329 Chlorophyll content of 4-day-old etiolated seedlings of Col-0, *glk1*, *glk2*, *glk1 glk2*,  
1330 *hy5*, *hy5 glk1*, *hy5 glk2*, and *hy5 glk1 glk2* grown on medium with or without 6-BA  
1331 during transition from dark to light conditions for 6 h (A) and 12 h (B). The data  
1332 represent means  $\pm$  SD (n=3) and letters above the bars indicate significant  
1333 differences ( $P < 0.05$ ), as determined by one-way ANOVA with Turkey's HSD test.  
1334 The experiments were performed three times with similar results.

1335

1336

1337

1338

1339

1340

1341

1342

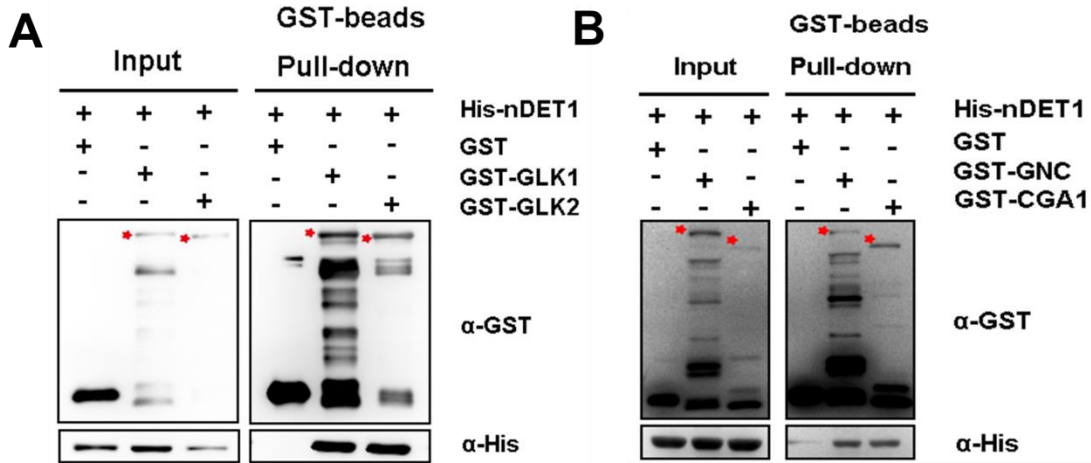
1343

1344

1345

1346





1366  
1367

1368 **Supplemental Figure S8.** *In vitro* evidence of DET1 interacting with GLK and  
1369 GNC/CGA1 proteins.

1370

1371 *In vitro* pulldown assays showing the interactions of GLK1, GLK2 (A), GNC and  
1372 CGA1 (B) with DET1. GST-GLK1, GST-GLK2, GST-GNC, GST-CGA1 or GST  
1373 proteins were used to pull down His-nDET1 protein using GST beads. Anti-GST  
1374 and anti-His antibodies were used for immunoblot analysis. “-” and “+” indicate the  
1375 absence and presence of corresponding proteins.

1376  
1377